cosmetics

MDPI

Article

Collagen and Hyaluronic Acid Combinations Modulate Intestinal Barrier Function and Skin Extracellular Matrix Responses in a Gut–Skin In Vitro Model

Francesca Parini [1], Matteo Musu [2], Rebecca Galla [1], Simone Mulè [2] and Francesca Uberti [2,*]

[1] Noivita s.r.l.s., Spin Off of University of Piemonte Orientale, Strada Privata Curti n. 7, 28100 Novara, Italy; francescaparini00@gmail.com (F.P.); rebecca.galla@noivita.it (R.G.)
[2] Laboratory of Physiology, Department for Sustainable Development and Ecological Transition, University of Piemonte Orientale (UPO), 13100 Vercelli, Italy; 20049586@studenti.uniupo.it (M.M.); simone.mule@uniupo.it (S.M.)
* Correspondence: francesca.uberti@uniupo.it

Abstract

Collagen and hyaluronic acid (HA) are major extracellular matrix (ECM) components involved in skin structure and tissue homeostasis. However, the biological effects of different collagen sources, when combined with HA, following intestinal passage, remain incompletely characterised. This study investigated the effects of bovine and marine collagen hydrolysates and a compositionally distinct biomimetic formulation, each combined with two distinct HA preparations (such as GreenIuronic® and sodium hyaluronate), in an integrated gut–skin in vitro model. Caco-2 intestinal cells were used to assess barrier integrity, fluorescein permeability, basolateral recovery of the measured analytes, oxidative stress and tight junction-related proteins. A skin co-culture model was subsequently exposed to basolateral medium collected from treated Caco-2 cultures and analysed for cell viability and ECM-related endpoints. The tested combinations generally improved transepithelial electrical resistance, passage through the intestinal model, cell viability, and tight junction protein expression compared with untreated controls. Following exposure to basolateral medium collected from treated Caco-2 cultures, the skin co-culture model showed changes in ECM-related measurements, including collagen, elastin and measured HA levels. Combinations containing GreenIuronic® were generally associated with stronger effects under the experimental conditions tested. Western blot analyses further supported modulation of ECM-related proteins, including COL1A1, HAS2, ELN, and MMP1, suggesting a shift towards a matrix-supportive profile. In conclusion, these findings provide preliminary in vitro evidence that collagen-HA combinations may modulate intestinal barrier-related parameters and extracellular matrix-associated measured endpoints within an integrated gut-skin model.

Keywords: gut–skin interaction; collagen peptides; hyaluronic acid; extracellular matrix; biomimetic formulation; skin homeostasis; skin physiology; nutraceuticals

Check for updates

Academic Editor: Gustavo Facchini

Received: 20 August 2026
Revised: 14 October 2026
Accepted: 15 October 2026
Published: 29 October 2026

Copyright: © 2026 by the authors. Licensee MDPI, Basel, Switzerland. This article is an open access article distributed under the terms and conditions of the Creative Commons Attribution (CC BY) license.

1. Introduction

Collagen is the most abundant protein in the mammalian extracellular matrix (ECM), accounting for approximately 30% of total body proteins and providing mechanical strength to connective tissues such as skin, cartilage, tendons, and bones [1]. In addition to its mechanical role, collagen participates in a variety of biological processes by regulating

cell adhesion, proliferation, migration, and differentiation through binding to cell-surface receptors, including integrins and discoidin domain receptors [2]. Because of these properties, collagen has attracted considerable interest in biomedical, dermatological, and nutritional research, particularly in studies focusing on connective tissue physiology, skin health, and extracellular matrix remodelling [3]. In recent years, collagen has also been widely investigated as a bioactive component in nutraceutical formulations to support connective tissue and skin physiology [4]. Experimental and clinical studies suggest that collagen-derived compounds may influence cellular responses involved in extracellular matrix metabolism, including collagen synthesis and tissue regeneration processes [5]. In vitro models have therefore been extensively used to investigate the biological activity of collagen and collagen-derived preparations, providing controlled systems to explore their effects on cellular viability, proliferation, and extracellular matrix-related pathways [6]. These models have contributed to understanding how collagen-derived compounds may influence cellular processes involved in connective tissue homeostasis [2]. Cellular studies have shown that collagen exposure can modulate processes involved in extracellular matrix production, fibroblast activation, and tissue repair. These studies suggest that collagen-derived compounds may modulate pathways involved in connective tissue homeostasis and tissue remodelling [7,8].

Collagen used in biomedical and nutraceutical applications can be derived from different sources, including terrestrial animals (e.g., bovine and porcine), marine organisms (e.g., fish skin and scales), and, more recently, alternative non-animal sources such as recombinant or plant-based collagen-like proteins. These sources have distinct biochemical and biophysical properties, including differences in molecular weight, amino acid composition, thermal stability, and bioavailability, which may affect their biological activity [9,10]. For example, compared with mammalian collagen, marine-derived collagen often has lower thermal stability but higher bioavailability due to its lower molecular weight and degree of crosslinking [11]. On the other hand, because of their structural resemblance to human collagen, bovine and porcine collagens have been investigated more thoroughly and utilised extensively; nonetheless, concerns about immunogenicity, disease transmission, and sustainability have prompted the search for alternative sources [12].

In this context, the synthesis of collagen-mimetic or plant-derived collagen-like materials has shown promise in addressing some of the drawbacks of animal-derived collagen. These biomimetic systems have been proposed as potentially more sustainable and standardisable alternatives to animal-derived collagen preparations while replicating important structural and functional characteristics of natural collagen, such as triple-helix organisation and the capacity to interact with biological receptors [13]. However, despite growing interest, limited data are available on their biological equivalence or potential functional similarities to traditional animal-derived collagen, particularly when combined with other ECM components.

Alongside collagen, hyaluronic acid (HA) represents another major component of the extracellular matrix. HA is a linear, non-sulfated glycosaminoglycan composed of repeating disaccharide units of glucuronic acid and N-acetylglucosamine [14]. Due to its high molecular weight and hydrophilic nature, HA can bind large quantities of water, thereby contributing to tissue hydration, viscoelasticity, and mechanical resilience. In the skin and other connective tissues, HA plays a crucial role in maintaining extracellular matrix organisation and facilitating cellular communication. HA also participates in several physiological processes, including wound healing, modulation of inflammation, and tissue remodelling [15]. These functions are mediated by interactions with cell-surface receptors such as CD44 and RHAMM, which regulate intracellular signalling pathways associated with cell proliferation, migration, and extracellular matrix production. As a result, HA

has become a widely investigated biomolecule in regenerative medicine, dermatology, and nutraceutical research [16]. Numerous in vitro studies have examined the biological effects of HA on fibroblasts and other connective tissue cells. For example, treatment of cultured human fibroblasts with HA-based formulations has been shown to stimulate extracellular matrix production and promote collagen synthesis [17]. In dermal fibroblast cultures, HA exposure has been associated with increased expression of type I collagen and enhanced matrix deposition, suggesting a role in stimulating neocollagenesis and improving tissue regeneration processes [18]. Similarly, HA has been shown to increase cell viability and proliferation in tendon-derived cells and to promote collagen type I expression, highlighting its capacity to influence ECM metabolism and connective tissue repair [19]. The biological effects of HA appear to be influenced by several factors, including molecular weight, concentration, and the cellular context in which it is applied [20]. Different molecular weight HA preparations have demonstrated variable effects on fibroblast proliferation, apoptosis, and matrix synthesis, suggesting that HA may modulate cellular responses through multiple mechanisms. For instance, experimental studies have shown that HA can regulate collagen production and fibroblast activity in a dose-dependent manner in vitro [19]. Given that collagen and HA naturally coexist within the extracellular matrix, increasing attention has been directed toward their combined use in cell culture models. The combination of these two ECM components has been proposed to better reproduce the native microenvironment of connective tissues and to modulate biological responses associated with extracellular matrix homeostasis [21].

Recent studies have suggested that the combination of collagen and HA may enhance biological responses compared with either component alone [22]. In cellular models, combinations of these molecules have been reported to influence extracellular matrix–related pathways, modulate inflammatory responses, and support cellular processes involved in tissue regeneration [23].

These findings suggest that the combined use of collagen and HA may provide a more physiologically relevant context for modulating cellular activity associated with connective tissue function. Despite the increasing interest in collagen and HA as bioactive compounds in biomedical and nutraceutical applications, limited information is available on how different collagen preparations interact with HA to modulate cellular responses relevant to intestinal and skin physiology within integrated in vitro systems [21]. Therefore, the present study comparatively evaluated bovine and marine collagen hydrolysates and a compositionally distinct biomimetic formulation, both alone and in combination with distinct HA formulations, within a gut–skin in vitro model. The study specifically investigated intestinal barrier integrity, the dynamics of passage across the intestinal barrier (permeability), oxidative balance, and extracellular matrix-related responses following intestinal passage, with the aim of providing further mechanistic insight into the potential role of collagen- and HA-based combinations in extracellular matrix homeostasis.

2. Materials and Methods

2.1. Chemical Characterisation of the Collagen Hydrolysates and Biomimetic Formulation

2.1.1. Determination of Total Protein

The total protein content was determined using the Kjeldahl method, which quantifies the total nitrogen in the matrix [24]. In summary, 0.5 g of each sample was subjected to digestion with concentrated sulfuric acid in the presence of a catalyst, with the aim of converting the organic nitrogen into ammonium ions. Subsequently, the digestate was mixed with NaOH (Merck Life Science, Rome, Italy), thereby converting the ammonium into ammonia. The presence of ammonia is then determined by titration with hydrochloric

acid. The nitrogen content was converted to protein using species-specific conversion factors [24], and the results were expressed as the mean ± SD (%) of protein by weight.

2.1.2. Determination of Protein Content by BCA Assay

The protein content present within the tested preparations was determined by means of the colourimetric BCA (bicinchoninic acid assay), which is based on the reduction of copper (Cu^{2+}) to Cu^{+} by peptide bonds [25]. The assay was performed using the Pierce™ BCA Protein Assay Kit (ThermoFisher Scientific, Waltham, MA, USA; Cat. No. 23225). Prior to analysis, samples were diluted 2-fold in ultrapure water. Bovine serum albumin (BSA) standards ranging from 0 to 200 µg/mL were prepared and analysed in parallel with the samples. Absorbance values (red at 562 nm with a spectrophotometer; Infinite 200 Pro MPlex, Tecan, Männedorf, Switzerland) were then subjected to correction using the reagent blank, and concentrations were subsequently calculated from the BSA calibration curve, with the necessary correction for the dilution factor. Samples generating signals outside the calibration range were diluted appropriately and re-analysed within the validated analytical range.

2.1.3. Determination of Hydroxyproline Content

The hydroxyproline content present within the tested preparations was determined by means of a colorimetric assay following acid hydrolysis. In summary, 10 mg of the sample was hydrolysed with 6 M HCl (Merck Life Science, Rome, Italy) at 110 °C for 24 h in sealed hydrolysis vessels. The resulting hydrolysates were appropriately diluted and reacted with chloramine-T, followed by Ehrlich's reagent containing p-dimethylaminobenzaldehyde (DMAB; Merck Life Science, Rome, Italy) for colour development. The absorbances were measured with a spectrophotometer at 558 nm (Infinite 200 Pro MPlex, Tecan, Männedorf, Switzerland). A seven-point calibration curve (0–20 µg/mL trans-4-hydroxy-L-proline; Merck Life Science, Rome, Italy) was prepared and processed in parallel with the samples. Subsequently, hydroxyproline concentrations were interpolated using the calibration curve and expressed as milligrams per gram of dry sample. The results were reported as the mean ± standard deviation from three independent hydrolysates, which were analysed in triplicate.

2.2. Agent Preparation

The study assessed the effects of bovine and marine collagen hydrolysates and a compositionally distinct biomimetic formulation on intestinal and skin-related endpoints. Bovine collagen consists of a highly purified preparation of hydrolysed collagen peptides obtained from bovine dermis through controlled enzymatic hydrolysis (GELITA AG, Eberbach, Germany; product No. 811012, batch No. 8222217), supplied by Vivatis Pharma GmbH (Hamburg, Germany). As stipulated by the manufacturer, the material comprises 91–95% protein on a dry-weight basis, with an average molecular weight of approximately 2 kDa, as determined by Tricine-SDS-PAGE molecular weight analysis. Marine collagen consists of bioactive hydrolysed collagen peptides obtained from marine fish sources through controlled enzymatic hydrolysis (GELITA AG, Eberbach, Germany; product No. 815131, batch No. FC220512G), supplied by Vivatis Pharma GmbH (Hamburg, Germany). The preparation exhibits physicochemical characteristics comparable to those of bovine collagen, including a protein content of approximately 91–95% on a dry-weight basis and an average molecular weight of approximately 2 kDa, as determined by Tricine-SDS-PAGE molecular weight analysis. The biomimetic preparation consisted of VeCollal® (TCI Co., Ltd., Taipei, Taiwan; product No. 30300103, batch No. 10073972), supplied by Vivatis Pharma GmbH (Hamburg, Germany). The material under discussion is derived exclusively from plant-

based, non-GMO ingredients and was developed as a non-animal alternative to collagen. In contrast to bovine and marine collagen, it is not an animal-derived collagen hydrolysate, but rather a proprietary biomimetic formulation comprising selected amino acids, vitamin C, Centella asiatica extract and Panax ginseng extract. This formulation has been designed to mimic specific compositional and functional features associated with human type I collagen, with a view to supporting endogenous collagen synthesis pathways.

All three preparations were evaluated at concentrations ranging from 50 to 500 µg/mL, based on previously published in vitro studies [26,27] and preliminary dose-response experiments conducted in the present model.

Two distinct hyaluronic acid formulations were subsequently appraised in conjunction with the selected concentrations of the three preparations. GreenIuronic® (Vivatis Pharma GmbH, Hamburg, Germany; CAS No. 778577-37-0; batch No. YET250224W28-01) was a patented, non-animal-derived hyaluronic acid ingredient that is obtained from *Tremella fuciformis* through an aqueous extraction and purification process. Confirmatory analyses, based on the corresponding certificate of analysis and manufacturer documentation, indicated a hyaluronic acid content of 92.9 ± 1.84% and a molecular-weight range of approximately 2000–4000 kDA, as determined by agarose gel electrophoresis. Fermentation-derived sodium hyaluronate (Xinjiang Fufeng Biotechnologies Co., Ltd., Urumchi, China; CAS No. 9067-32-7; batch No. HA2025041527X), supplied by Vivatis Pharma GmbH (Hamburg, Germany), consists of sodium hyaluronate powder obtained by microbial fermentation. Confirmatory analyses, based on the corresponding certificate of analysis and manufacturer documentation, indicated a sodium hyaluronate content of 87.6 ± 1.75% and a molecular-weight range of approximately 300–500 kDA, as determined by agarose gel electrophoresis.

Subsequently, the selected concentrations for each of the three preparations were tested in combination, at full and half doses, with two different forms of hyaluronic acid. Specifically, non-animal hyaluronic acid (GreenIuronic®, designated GI, donated by Vivatis Gmbh, Hamburg, Germany) and fermentation hyaluronic acid (sodium hyaluronate, designated SH) were utilised at a concentration of 10 µg/mL [4,28].

All compounds were directly dissolved in phenol-red-free Dulbecco's Modified Eagle's Medium (DMEM, Merck Life Science, Rome, Italy) with the addition of 0.5% foetal bovine serum (FBS, Merck Life Science, Rome, Italy), 2 mM L-glutamine (Merck Life Science, Rome, Italy), and 1% penicillin-streptomycin (Merck Life Science, Rome, Italy) and diluted in order to obtain the final concentration in the well.

All physicochemical characteristics, compositional specifications, molecular-weight ranges and formulation information for the tested materials were obtained from the respective manufacturers' technical data sheets and certificates of analysis associated with the batches used in this study. In order to provide further support for material characterisation, the hydroxyproline content was experimentally determined and is reported in the main manuscript. Supplementary Figures S1 and S2 and Supplementary Tables S1 and S2 contained the complete physicochemical characterisation of the tested materials. Further physicochemical characterisation, incorporating Tricine-SDS-PAGE profiles, pH measurements, aqueous soluble fraction data, compositional analysis by the glucuronic acid method and agarose gel electrophoresis profiles of the hyaluronic acid preparations, is presented in the Supplementary Materials (Supplementary Figures S1 and S2 and Supplementary Tables S1 and S2).

2.3. Cell Culture

The different compounds were tested on Caco-2, human intestinal epithelial cells (American Type Culture Collection, ATCC, Manassas, VA, USA) cultured in Advanced Dulbecco's Modified Eagle Medium (Adv-DMEM; GIBCO, Thermo Fisher Scientific, Waltham,

MA, USA), supplemented with 10% FBS, 2 mM L-glutamine (Merck Life Science, Rome, Italy), and 1% penicillin-streptomycin (Merck Life Science, Rome, Italy) and kept at 37 °C and 5% CO_2 [29]. Cells at passages 26–32 were used to maintain paracellular permeability integrity and transport properties comparable to those of the human intestine following oral intake. Cells were plated at different densities depending on the experimental purpose, including 1×10^4 cells per well in 96-well plates for cell viability by the (MTT)-based In Vitro Toxicology Assay Kit (Merck Life Science, Rome, Italy), and ROS levels were determined using cytochrome C (Merck Life Science, Rome, Italy) in complete culture medium. Furthermore, 2×10^4 cells were seeded onto 6.5 mm Transwell® inserts with a 0.4 µm pore polycarbonate membrane (Corning® Costar®, Merck Life Science, Rome, Italy) in 24-well plates to perform a permeability and integrity study by analysing TEER values and TJ protein levels [30]. Cells seeded on the Transwell® insert were maintained in complete medium and replaced every other day for 21 days to ensure maturation, which was considered complete when transepithelial resistance (TEER) reached ≥ 400 $\Omega \cdot cm^2$. Prior to Transwell® stimulation, the apical medium was adjusted to pH 6.5 to reproduce the pH of the small intestinal lumen, while the basolateral medium was maintained at pH 7.4 to mimic physiological blood conditions [30]. Before the viability assay, cells were incubated for 8 h in phenol red-free DMEM (Merck Life Science, Rome, Italy) with the addition of 0.5% foetal bovine serum (FBS, Merck Life Science, Rome, Italy), 2 mM L-glutamine (Merck Life Science, Rome, Italy), and 1% penicillin-streptomycin (Merck Life Science, Rome, Italy).

NHEK human epidermal keratinocytes (Lonza, Basel, Switzerland) were maintained in a keratinocyte basal medium (KBM medium, Lonza, Basel, Switzerland) that had been supplemented with keratinocyte growth supplements (KGM2, Lonza, Basel, Switzerland). These supplements comprised insulin, human epidermal growth factor, bovine pituitary extract, hydrocortisone, epinephrine, transferrin, and gentamicin/amphotericin B. The cells were cultivated until they reached 70–80% confluence in a controlled environment at 37 °C and 5% CO_2. Cells in the proliferative phase at passages between 2 and 3 were used for all experimental procedures to reproduce selected physiological characteristics of human epidermal tissue in vitro [28]. For the skin co-culture model, NHEK cells were seeded at a density of 3.8×10^4 in a 96-well plate to study cell viability by MTT-based In Vitro Toxicology Assay Kit (Merck Life Science, Rome, Italy) and oxidative stress through cytochrome C reduction assay; 1.5×10^5 in a 24-well plate to study intracellular pathways and quantify extracellular matrix components, including collagen types I, III, and IV and hyaluronic acid, together with ECM-related proteins assessed by Western blotting.

Primary adult dermal fibroblast (HDFa) cell line, purchased from ATCC (Manassas, VA, USA), was maintained in Fibroblast Basal Medium (Manassas, VA, USA) supplemented with fibroblast growth supplement (Manassas, VA, USA). For the experiments, cells were used after reaching a confluency of 70–80% [31] and were seeded at different densities for the skin co-culture model: 1×10^4 in a 96-well plate to study cell viability by MTT-based In Vitro Toxicology Assay Kit (Merck Life Science, Rome, Italy) and oxidative stress through the cytochrome C reduction assay (Merck Life Science, Rome, Italy). In addition, 5×10^4 in a 24-well plate to study intracellular pathways and quantify extracellular matrix components, including collagen types I, III, and IV and hyaluronic acid, together with ECM-related proteins assessed by Western blotting.

2.4. Experimental Protocol

The experiments were divided into two phases to assess intestinal responses to the tested preparations and subsequent skin co-culture responses following exposure to basolateral medium collected from treated Caco-2 cultures (Figure 1).

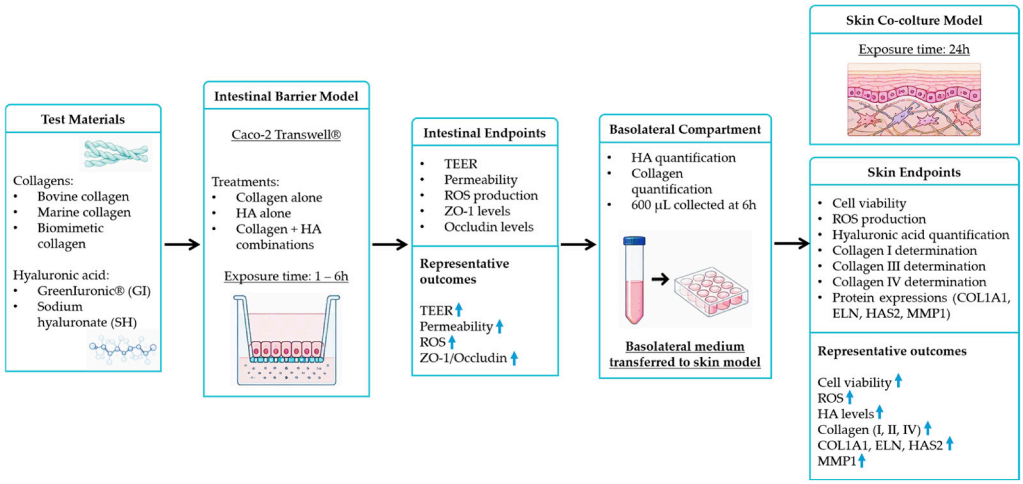


Figure 1. Experimental workflow of the integrated gut–skin model. Bovine and marine collagen hydrolysates and a compositionally distinct biomimetic formulation were tested individually or in combination with GreenIuronic® (GI) or sodium hyaluronate (SH) using an intestinal barrier model based on differentiated Caco-2 cells. After 6 h of treatment, the content of the basolateral compartment was collected, analyzed to determine the quantity of collagen and hyaluronic acid, and transferred (600 µL) onto a skin co-culture model consisting of NHEK keratinocytes and HDFa fibroblasts for 24 h. Subsequently, reference parameters relating to both the gut and the skin were evaluated.

In the first phase, a dose-response study at the intestinal level was conducted to determine which concentration of each of the three preparations exhibited the most suitable biological profile under the experimental conditions tested, with a treatment interval of 1–6 h. Subsequently, an in vitro intestinal model was created to study the paracellular permeability and the intestinal integrity of orally taken compounds after treatment with the three preparations at the selected full dosage of 200 µg/mL and half dosage of 100 µg/mL, both singular and combined with two different hyaluronic acids, GI and SH, prepared at a concentration of 10 µg/mL. To evaluate potential combined effects. Therefore, the integrity of the cellular monolayer was assessed by measuring TEER, and permeability was measured using a fluorescent probe over 1–6 h following stimulation to mimic intestinal transit, thereby calculating Jmax [32]. Cell viability (assessed by the MTT assay) and reactive oxygen species (ROS, evaluated via a cytochrome C reduction assay) were assessed after a 6-h treatment with the compounds. Following this step, in the same in vitro model, the three preparations and the two HA formulations were tested individually and in combination to assess intestinal integrity using the TJ ELISA kit (ZO-1 and Occludin; MyBiosource, San Diego, CA, USA) [30]. In addition, the amount of hyaluronic acid, collagen, hyaluronan and hydroxyproline was evaluated at the end of 6 h of treatment in the basolateral compartment.

In the subsequent phase of the study, responses to basolateral medium collected from treated Caco-2 cultures were examined using the skin co-culture model in 24-well plates. This experimental design linked the intestinal barrier model to the skin co-culture model through the transfer of basolateral medium. The tested preparations, individually or in combination, were applied to the intestinal cells in the apical compartment of the Transwell system. Subsequently, the basolateral material was collected and utilised for a 24-h treatment of the skin co-culture model, with the objective of assessing cell viability (via the MTT assay) and ROS production (via cytochrome c reduction). For each experimental condition, 600 µL of basolateral medium was collected immediately after the conclusion of the 6-h intestinal treatment and transferred directly to the skin co-culture model without any dilution, concentration, or additional pretreatment. The collected basolateral medium was maintained under the same experimental conditions for all groups and applied to the skin

co-culture model for 24 h. Control skin co-cultures were provided with basolateral medium collected from untreated Caco-2 cells, thus enabling a comparison of all experimental groups under identical transfer conditions. Intracellular pathways and extracellular matrix components, including collagen types I, III, and IV and hyaluronic acid, together with ECM-related proteins assessed by Western blotting, were analysed.

2.5. Intestinal Barrier In Vitro Model

This study was designed to assess intestinal barrier function and basolateral recovery of the measured analytes following exposure to the tested preparations. Following a well-established protocol reported in the literature and recognised by both the European Medicines Agency (EMA) and the Food and Drug Administration (FDA), an in vitro intestinal barrier model was established using a Transwell® system to investigate transepithelial transport, passage across the intestinal epithelial model, and barrier-related parameters under in vitro conditions.

At the beginning of the experiment, Caco-2 cells were seeded according to validated protocols and maintained in complete medium for 21 days. During this period, the culture medium was regularly refreshed in both the apical and basolateral compartments to support optimal cell growth and differentiation, thereby preserving monolayer integrity and reproducing the physiological conditions necessary for subsequent experiments [33]. After TEER values reached a minimum of 400 $\Omega \cdot cm^2$ on day 21, permeability studies were initiated. Permeability was assessed through the utilisation of 0.04% fluorescein as a paracellular fluorescent tracer (Merck Life Science, Rome, Italy; product number 46955). Fluorescence was measured at excitation/emission wavelengths of 490/514 nm following sample processing, and this was used as an indirect indicator of transepithelial permeability, rather than measuring collagen or hyaluronic acid transport directly. The fluorescence-based permeability tests and the subsequent biochemical analyses of basolateral samples were conducted using the same Transwell® inserts. The cells were exposed to the test compounds for a period of 1 to 6 h prior to analysis. Prior to Transwell® treatment, the apical medium was adjusted to pH 6.5 to simulate the small intestinal environment, while the basolateral medium was adjusted to pH 7.4 to reflect physiological blood conditions [34]. The test preparations were administered to the apical compartment in a final volume of 200 µL, while the basolateral compartment contained 600 µL of medium. To ensure stability of that condition, the cells were kept for 15 min at 37 °C and 5% CO_2. In order to evaluate the permeation rate (nmol min/mg protein), J was calculated using a validated formula [35]:

$$J = (Jmax \times [C])/(Kt + [C])$$

where:

C = starting concentration of fluorescein.

Jmax = maximum permeation rate.

Kt represents the Michaelis–Menten constant.

Results are expressed as mean ± SD (% relative to untreated control cells). Cell-free negative controls were examined to rule out Transwell® membranes.

In order to assess the direct passage of the compounds across the intestinal barrier, the concentrations of hyaluronic acid, collagen, hyaluronan and hydroxyproline in the basolateral compartment were quantitatively analysed after 6 h of treatment. Basolateral samples were collected and analysed using specific ELISA assays. However, they are unable to provide information regarding molecular weight distribution, structural integrity, or the identity of individual transported species. These measurements were utilised to assess the transfer of the substances under investigation across the intestinal model under the experimental conditions examined. Additional aliquots of basolateral medium were

analysed for hyaluronan and total hydroxyproline as complementary biochemical markers of the recovered material. The corresponding results are presented in Appendix B, Tables A1 and A2.

2.6. Skin Co-Culture Model

To replicate interactions between the epidermis and dermis in vitro and to explore the effects of treatments, a co-culture model comprising NHEK and HDFa cells was used, as reported in the literature [36]. The protocol involved the use of 5% gelatin hydrogel (scaffold, Nitta Gelatin Inc., Osaka, Japan) used in multi-well plates to recreate the co-culture model in vitro following an HDFa/NHEK cell density ratio of 1:3. With regard to the experimental procedure, HDFa cells were seeded on the 5% gelatin scaffold, which had been added to the well, and maintained for 3 days under these culture conditions. Subsequently, NHEK keratinocytes were added to recreate the co-culture, maintaining a 1:3 ratio. In order to conduct a study on gut–skin interaction, 600 µL of basolateral medium collected after a period of 6 h of treatment in the intestinal barrier model was transferred directly into the skin co-culture model, without the need for dilution or further processing. The skin co-cultures were exposed to the transferred medium for a period of 24 h prior to analysis. Each condition was tested in triplicate across five independent experiments. Control skin co-cultures were provided with basolateral medium obtained from untreated Caco-2 cells and processed under identical experimental conditions.

2.7. In Vitro Toxicology Assay Kit

Cell viability in both gut cells and the skin co-culture model was evaluated using the In Vitro Toxicology Assay Kit (Merck Life Science, Rome, Italy) according to previously validated protocols [34]. Absorbance was measured at 570 nm with background correction at 690 nm using a spectrometer (Infinite 200 Pro MPlex, Tecan, Männedorf, Switzerland), and results were normalised to untreated controls. Data are expressed as mean ± SD (%) from five independent experiments performed in triplicate.

2.8. ROS Production

The levels of ROS produced in both treated and untreated cells were determined by cytochrome C reduction [37] in both gut cells and the skin co-culture model. Briefly, 100 µL of superoxide dismutase and 100 µL of cytochrome C (Merck Life Science, Rome, Italy) were added to the cells, which were then incubated at 37 °C and 5% CO_2 for 30 min. Absorbance was measured at 550 nm using a spectrometer (Infinite 200 Pro MPlex, Tecan, Männedorf, Switzerland). Results are expressed as mean ± SD (%) relative to control from five independent experiments performed in triplicate.

2.9. Human ZO-1 ELISA Kit

ZO-1 levels in Caco-2 cell lysates were quantified using a Human Tight Junction Protein 1 ELISA kit (MyBiosource, San Diego, CA, USA) according to the manufacturer's instructions [29]. Briefly, samples (100 µL) were incubated at 37 °C, followed by sequential incubations with Detection Solution A and B, substrate addition, and reaction stop. Absorbance was read at 450 nm using a spectrophotometer (Infinite 200 Pro MPlex, Tecan, Männedorf, Switzerland). Results were expressed in pg/mL using a 0–1000 pg/mL standard curve and reported as mean ± SD from five independent experiments performed in triplicate, relative to the control.

2.10. Human Occludin ELISA Kit

Occludin levels in Caco-2 cell lysates were determined using a Human Occludin ELISA kit (MyBiosource, San Diego, CA, USA) following the manufacturer's instructions [29]. In summary, 100 µL of the sample was incubated at 37 °C and 5% CO_2 for 90 min, followed by sequential treatment with Detection Solution A and B, substrate addition, and reaction stop. Absorbance was measured at 450 nm using a spectrophotometer (Infinite 200 Pro MPlex, Tecan, Männedorf, Switzerland). Data were expressed as pg/mL (standard curve ranging from 0 to 1000 pg/mL) and were reported as the mean ± SD, derived from five independent experiments, each performed in triplicate, compared to the control.

2.11. Collagen Type I Quantification

Collagen type I levels were measured in lysates from the skin co-culture model using a colourimetric assay kit (Abcam, San Diego, CA, USA), following the manufacturer's instructions. Briefly, 100 µL of each sample was dispensed into a 96-well plate and incubated at 65 °C with the Reaction Mix until the samples had completely evaporated. Subsequently, 100 µL of Oxidation Mix was added, and samples were incubated for 20 min at room temperature. Thereafter, 50 µL of Developer was introduced and incubated at 37 °C for 5 min. Finally, 50 µL of DMAB reagent was added, and the plate was incubated at 65 °C for 45 min, protected from light. Absorbance was measured at 560 nm using a spectrophotometer (Infinite 200 Pro MPlex, Tecan, Männedorf, Switzerland). The basolateral samples were diluted 1:10 and reanalyzed. Final concentrations were calculated after correction for the corresponding dilution factor and are expressed in µg/mL of the original basolateral medium (Table A1). Data were expressed as mean ± SD (% relative to control), and concentrations (pg/mL) were calculated from a standard curve (0.5–10 µg).

2.12. Collagen Type III Quantification

Skin co-culture model lysates were used to quantify type III collagen using the Human COL3 (Collagen Type III) ELISA Kit from FineTest (Fine Biotech Co., Wuhan, China), according to the manufacturer's instructions [38]. Absorbance values were recorded at 450 nm using a spectrophotometer (Infinite 200 Pro MPlex, Tecan, Männedorf, Switzerland). Results were reported as mean ± SD (% vs. control), and concentrations (ng/mL) were extrapolated from a standard curve ranging from 0.625 to 40 ng/mL.

2.13. Collagen Type IV Quantification

Collagen type IV levels were assessed in lysates from the skin co-culture model using the Human COL4 (Collagen Type IV) ELISA Kit from FineTest (Fine Biotech Co., Wuhan, China), according to the manufacturer's instructions [39]. Absorbance was determined at 450 nm using a spectrophotometer (Infinite 200 Pro MPlex, Tecan, Männedorf, Switzerland). Data were presented as mean ± SD (% of control), and collagen concentrations (ng/mL) were calculated from a standard curve ranging from 0.781 to 50 ng/mL.

2.14. Hyaluronic Acid ELISA Kit

Total hyaluronic acid levels in skin co-culture model and intestinal cell lysates were quantified using a Hyaluronic Acid ELISA kit (CloudClone, Houston, TX, USA) according to the manufacturer's instructions [40]. The samples were appropriately diluted at a ratio of 1:10, and the final concentrations were adjusted according to the dilution factor. Specifically, the data, which were initially measured in ng/mL, were converted to µg/mL to ensure consistency in presenting data on basolateral measurements and the initial dosage (Table A1). Absorbance was measured at 450 nm using a spectrophotometer (Infinite 200

Pro MPlex, Tecan, Männedorf, Switzerland), and results are expressed as mean ± SD (%) relative to the control from five independent experiments performed in triplicate.

2.15. Western Blot Analysis

Protein expression of collagen type I alpha 1 chain (COL1A1), hyaluronan synthase 2 (HAS2), elastin (ELN), and matrix metalloproteinase-1 (MMP1) was evaluated in skin co-culture model lysates following exposure to basolateral medium collected from treated Caco-2 cultures. The expected molecular weights of the analysed proteins were approximately 90 kDa for COL1A1, 63 kDa for HAS2, 55 kDa for ELN, 52 kDa for MMP1, and 42 kDa for β-actin. Uncropped and annotated blots are available in the supplementary material. Cells were lysed using Radioimmunoprecipitation assay (RIPA) lysis buffer supplemented with protease and phosphatase inhibitors (Merck Life Science, Rome, Italy). Total protein concentration was quantified using the Bradford assay (Bio-Rad Laboratories, Hercules, CA, USA). Equal amounts of protein (20–30 µg) were separated by Sodium Dodecyl Sulphate–Polyacrylamide Gel Electrophoresis (SDS–PAGE) and transferred onto polyvinylidene fluoride (PVDF) membranes (GE Healthcare Europe GmbH, Milan, Italy) membranes. Membranes were blocked with 5% non-fat milk in Tris-buffered saline with Tween-20 (TBS-T; Merck Life Science, Rome, Italy) and incubated overnight at 4 °C with primary antibodies against COL1A1, HAS2, ELN, and MMP1 (1:500; Santa Cruz Biotechnology, Santa Cruz, CA, USA). After incubation with HRP-conjugated secondary antibody, anti-mouse IgG (1:5000; Merck Life Science, Rome, Italy), protein bands were visualised using enhanced chemiluminescence. β-actin (Merck Life Science, Rome, Italy) was used as a housekeeping protein for normalisation. Band intensity was quantified using Image LabTM Software version 5.2.1 (Bio-Rad, Hercules, CA, USA). Data are expressed as mean ± SD (% relative to untreated control cells) from three independent experiments performed in triplicate.

2.16. Hyaluronan ELISA Kit

The concentrations of hyaluronan in the basolateral samples were determined using the Hyaluronan Enzyme-Linked Immunosorbent Assay Kit (Echelon Biosciences, Salt Lake City, UT, USA; K-1200). This process was conducted in accordance with the manufacturer's instructions. Samples (100 µL) were analysed in duplicate, and the absorbances were measured at 405 nm. The concentrations were calculated using the supplied hyaluronan standard curve (50–1600 ng/mL). The samples were diluted 1:10, and the final concentrations were corrected based on the corresponding dilution factor. The concentrations were then converted to µg/mL for data reporting purposes (Table A2). The results obtained are expressed as mean values, which were obtained from five independent experiments that were performed in triplicate.

2.17. Hydroxyproline Determination

The total hydroxyproline concentrations in the basolateral samples were determined using the QuickZyme Hydroxyproline Assay Kit (QuickZyme Biosciences, Leiden, The Netherlands; QZBhypro1). This was done in accordance with the instructions provided by the kit manufacturer. Prior to analysis, samples were subjected to acid hydrolysis and subsequently quantified against the hydroxyproline calibration curve supplied with the kit (0.8–39.3 µg/mL). The samples were diluted 1:10 and the final concentrations corrected according to the dilution factor. These concentrations were then converted to µg/mL for reporting purposes (Table A2). The results obtained are expressed as mean values obtained from five independent experiments performed in triplicate.

2.18. Statistical Analysis

The results of all experimental analyses, except for Western blot, were presented as the mean ± standard deviation (SD) of five independent biological experiments, each of which was performed in technical triplicate. For each experiment, the technical replicates were averaged to obtain a single value, and statistical analyses were conducted using the resulting biological replicate values ($n = 5$). Western blot data were presented as the mean ± SD of three independent biological experiments, each analysed in technical triplicate. Similarly, the technical replicates were averaged prior to statistical analysis, and the biological experiments were treated as the statistical unit for all statistical analyses ($n = 3$). Representative blots are included. Before proceeding to the statistical analysis, the normality and homogeneity of variance were assessed using the Shapiro-Wilk and Brown-Forsythe tests, respectively. Statistical analysis was conducted using a one-way ANOVA, followed by a Bonferroni post hoc test, in GraphPad Prism 10.2.3 (GraphPad Software, La Jolla, CA, USA). The level of statistical significance was defined as $p < 0.05$. Data were normalised to untreated control cells and expressed as mean ± SD (% relative to control). Bonferroni's correction was applied to account for multiple comparisons. Except for the direct GI–SH comparisons reported in Appendix B (Tables A3–A5), statistical comparisons were performed using one-way ANOVA followed by Bonferroni's multiple-comparison test. To facilitate the direct comparison between GreenIuronic® and sodium hyaluronate, additional quantitative analyses were performed for selected skin-related endpoints (COL1A1, HAS2 and MMP1). Tables A3–A5 report the mean values and standard deviations for each formulation, the mean differences between GI and SH with their 95% confidence intervals, and the adjusted p-values. Direct comparisons between GI- and SH-containing formulations reported in Appendix B (Tables A3–A5) were performed using one-way ANOVA followed by Tukey's multiple-comparison test. The reported p-values were adjusted using Tukey's procedure, and adjusted p-values < 0.05 were considered statistically significant. The meaning of all statistical symbols used in the figures is specified in the corresponding figure legends.

3. Results

3.1. Analysis of Protein and Hydroxyproline Content in the Collagen Hydrolysates and Biomimetic Formulation

Prior to commencing the biological experiments, an analysis was conducted to ascertain the protein content of the bovine and marine collagen hydrolysates and the biomimetic formulation, with a view to determining whether there were any differences in protein content. In the initial phase of the study, two methodologies were employed to ascertain protein content: the Kjeldahl method and the BCA method. As demonstrated in Table 1, the data obtained by the Kjeldahl method revealed significant variations in protein content among the tested preparations. Specifically, the data showed comparable protein content between Bovine collagen (approximately 91.7%) and Marine collagen (approximately 92.8%), whereas the biomimetic formulation had a lower protein content (approximately 74.2%). To verify these data, the BCA assay was also performed to determine protein content. In accordance with the preceding observations, this test further corroborates the similarity in protein content between Bovine collagen (92.5%) and Marine collagen (93.6%), while the biomimetic formulation exhibited a reduced protein content (approximately 75.4%).

Table 1. Determination of protein content in the bovine and marine collagen hydrolysates and the biomimetic formulation. Data are expressed as mean (%) ± SD of five independent experiments, each performed in triplicate.

Sample	Kjeldahl Method	BCA assay	Chloramine-T/DMAB Assay
	Protein Content (%)	Protein Content (%)	Hydroxyproline Content (%)
Bovine collagen	91.7 ± 1.23	92.5 ± 1.78	11.9 ± 0.49
Marine collagen	92.8 ± 1.27	93.6 ± 1.95	11.4 ± 0.42
Biomimetic formulation	74.2 ± 1.19	75.4 ± 1.62	0.80 ± 0.11

In order to provide a more detailed characterisation of the materials that were tested, the level of hydroxyproline was measured as a marker of composition. Bovine and marine collagen displayed similar hydroxyproline contents (11.9 ± 0.3% and 11.4 ± 0.4% w/w, respectively), whereas the biomimetic preparation contained substantially lower levels (0.8 ± 0.2% w/w). These results are consistent with the collagen-derived origin of the bovine and marine preparations and highlight the distinct compositional profile of the biomimetic material.

3.2. Effects of the Tested Preparations on Caco-2 Cell Responses and Barrier-Related Parameters

First, a preliminary screening was conducted to determine the optimal concentration for each tested preparation. At the intestinal level, cell viability was assessed after treatment with the tested preparations for exposure periods of 1 to 6 h at concentrations ranging from 50 to 500 µg/mL. The results presented in Figure A1 of Appendix A demonstrate that cells treated with each of the tested preparations, at the concentrations examined, showed increased cell viability compared with the untreated control (0% line, $p < 0.05$). Specifically, among the concentrations tested, 200 µg/mL was the most effective across all tested preparations ($p < 0.05$). Subsequently, intestinal barrier integrity was assessed by monitoring TEER values over 6 h in the Caco-2 Transwell system. As illustrated in Figure 2, the results showed that all tested agents, including marine and bovine collagen hydrolysates and the biomimetic formulation, maintained epithelial integrity relative to the control, with modest increases in TEER observed across several treatment conditions. Investigation of the individual agents (Figure 2A,C,E) revealed that half-dose combinations consistently yielded higher TEER values than full-dose combinations. For instance, in the case of Marine collagen (Figure 2A), the half-dose induced an improvement of approximately 4% over the control at the 4 h peak, whereas the full dose showed a more modest increase of about 2%. Furthermore, the combination of the tested preparations with hyaluronic acid derivatives (Figure 2B,D,F) appeared to have a significant impact on the TEER observed with the single agents. Specifically, the addition of GI was generally associated with stronger effects compared with SH under the tested experimental conditions. Also, in the biomimetic formulation group (Figure 2F), the combination with GI at a half-dose resulted in a substantial improvement of nearly 5% compared to the control ($p < 0.05$), outperforming the SH variant by roughly 1.5% at the same time point. Notably, while most agents peaked at 4 h, a decrease in TEER values was observed at 6 h. Even then, GI combinations remained roughly 2–3% above the baseline control. These findings indicate that the tested combinations modulated TEER values in the Caco-2 Transwell system, with GI-containing combinations generally showing higher values than the corresponding SH-containing combinations under the

experimental conditions tested. These observations provide a basis for further investigation of their potential relevance to intestinal barrier function and gut health.

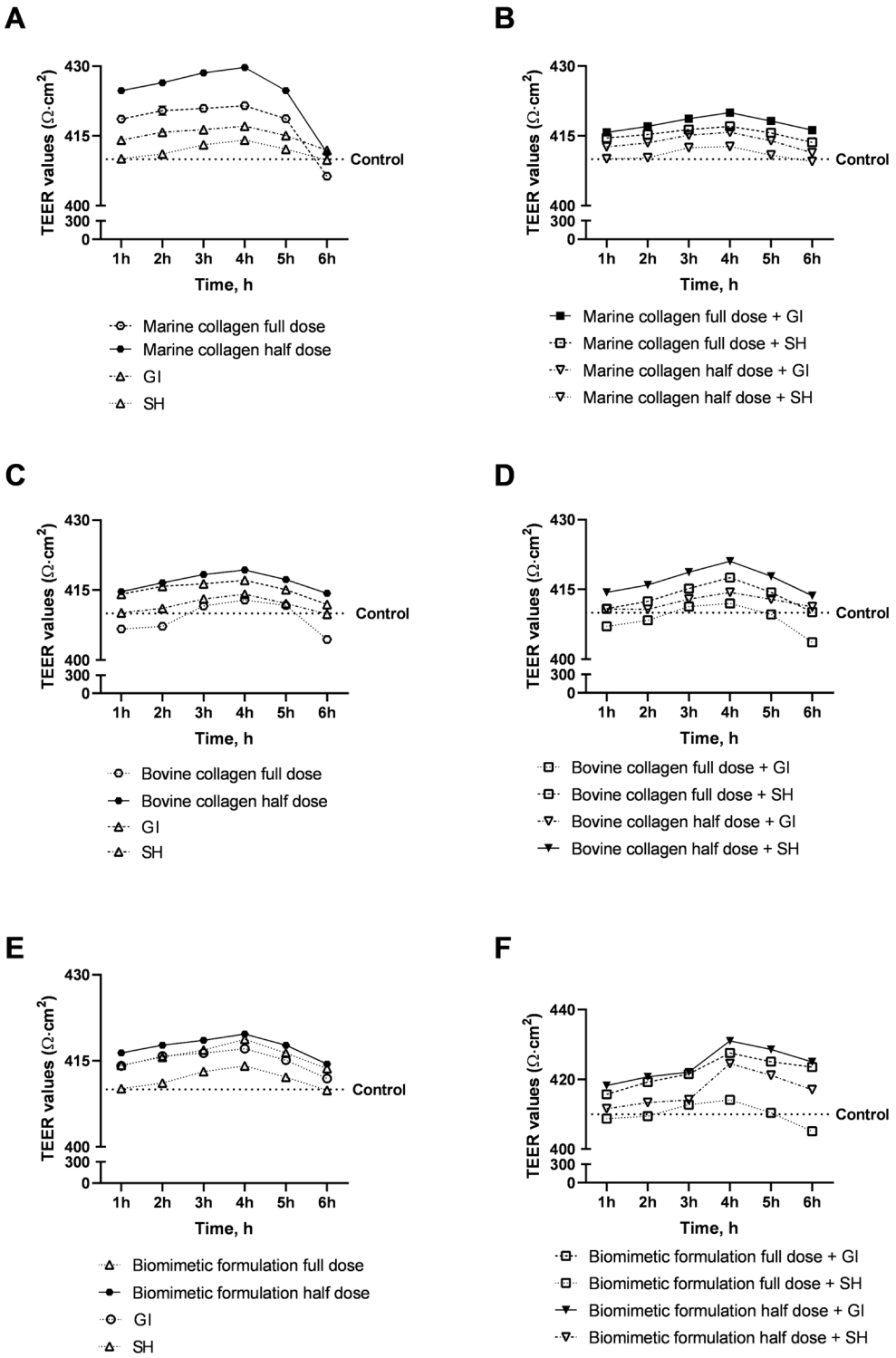


Figure 2. Assessment of intestinal barrier integrity in the Caco-2 Transwell system. In (**A**,**C**,**E**), TEER values measured using EVOM3 are reported for the individual preparations (marine and bovine collagen hydrolysates and the biomimetic formulation, at full and half doses) and for GI and SH. In (**B**,**D**,**F**), the TEER analysis of the respective combinations of the three preparations with GI or SH over a 6 h period was reported and evaluated by EVOM3. GI = GreenIuronic; SH = sodium hyaluronate. The dashed line represents the control values (about 410 ± 15 Ω·cm^2). Results are expressed as mean ± SD (%) of five independent experiments conducted in triplicate.

Intestinal barrier permeability (%) was further assessed using a fluorescein tracer in the Caco-2 Transwell system over a 6-h period. Fluorescein-based permeability measurements reached a maximum at 4 h and then gradually declined under the experimental conditions tested. Analysis of the individual components (Figure 3A,C,E) demonstrates that all tested agents showed increased transepithelial passage across the epithelial model, exhibiting significantly higher permeability than the control baseline. GI was generally associated with higher permeability values than SH under the experimental conditions tested. Specifically, Figure 3A showed that GI reached a peak permeability of approximately 44%, surpassing the SH variant by 10% ($p < 0.05$). Bovine collagen (Figure 2C) was associated with the highest transepithelial passage under the experimental conditions tested, with the half-dose reaching a peak of 55%, approximately 5% higher than the full-dose application ($p < 0.05$). In contrast, while the biomimetic formulation (Figure 3E) exhibited more modest independent permeability, quantified at approximately 10% compared to control ($p < 0.05$), its performance was significantly enhanced when administered in combination. Indeed, the enhancement observed in the combined combinations (Figure 3B,D,F) underscored a substantial improvement in transport across the intestinal barrier relative to single-agent treatments. The data further suggest that GI was generally associated with higher permeability values than SH under the experimental conditions tested ($p < 0.05$). Within the Marine collagen group (Figure 3B), the GI combination peaked at 30% compared to the control ($p < 0.05$), outperforming the SH counterpart by 6%. Similarly, in the biomimetic formulation group (Figure 3F), the half-dose, combined with GI, achieved a maximum of 24% compared to the control ($p < 0.05$) and the combination with SH ($p < 0.05$). Collectively, these results suggested that these combinations, particularly those incorporating GI, were associated with increased transport across the intestinal epithelial model, indicating that they may favour intestinal transport under the experimental conditions tested. In order to provide a more detailed interpretation of the transport data, further analyses were conducted by directly quantifying hyaluronic acid and collagen in the basolateral compartment. The results of these measurements are presented in Appendix B, Table A1, and provide further information regarding the material recovered in the basolateral compartment following passage through the intestinal barrier model. Further characterisation of the recovered material through hyaluronan and hydroxyproline determinations is reported in Appendix B, Table A2.

To provide a more comprehensive evaluation of the biocompatibility and antioxidant potential of the combinations, cell viability and ROS production in the intestinal model were assessed after 6 h of exposure. As demonstrated in Figure 4, all tested agents exhibited a favourable safety profile, with viability levels consistently remaining above the control baseline, indicating no cytotoxic effects. Furthermore, the investigation into oxidative stress revealed that most treatments reduced ROS production, consistent with a physiological pattern of cellular protection. MTT assay results (Figure 4A,C,E) showed higher values following treatment with GI than with SH under the experimental conditions tested. For instance, GI alone induced a 10% increase in viability compared to control ($p < 0.05$), while SH showed a more modest 5% increase ($p < 0.05$). Among the tested preparations, the biomimetic formulation at half-dose (Figure 4E) demonstrated the most significant impact, boosting viability by approximately 20% compared to the control ($p < 0.05$). When administered in combination, a clear enhancing effect was observed. Notably, the combination of the biomimetic formulation at half-dose with GI achieved the highest viability peak, nearly 30%, compared to the control ($p < 0.05$), outperforming the SH counterpart by over 10% ($p < 0.05$). Regarding the antioxidant activity (Figure 4B,D,F), the data confirm that these combinations significantly mitigate oxidative stress compared with the control ($p < 0.05$). GI was generally associated with greater reductions in ROS levels than SH across the tested

groups. In the biomimetic formulation series (Figure 4F), the combination with GI induced a substantial reduction in ROS production, reaching approximately -10% relative to the control ($p < 0.05$), whereas the SH variant achieved only −2%. While Bovine collagen (Figure 4D) initially showed a slight increase in ROS when administered alone, the addition of GI successfully reversed this trend, bringing ROS levels back toward a protective state ($p < 0.05$). Collectively, these results suggest that GI-containing combinations were associated with greater preservation of cellular viability and lower ROS levels under the experimental conditions tested.

To complement the TEER measurements, the expression levels of key TJ proteins, specifically Occludin and Zo-1, were quantified after 6 h of exposure. As demonstrated in Figure 5, all tested agents significantly upregulated the expression of these proteins relative to the control baseline ($p < 0.05$), supporting the modulation of molecular markers associated with intestinal barrier integrity. In accordance with the previously discussed permeability and integrity data, GI consistently enhanced TJ protein levels compared to the SH ($p < 0.05$). Analysis of Occludin levels (Figure 5A,C,E) revealed that Marine collagen (Figure 5A) and Bovine collagen (Figure 5C) both effectively supported protein expression. Especially, in the Bovine group, the half-dose combined with GI achieved about 16% increase compared to control ($p < 0.05$), notably outperforming the full-dose combination ($p < 0.05$). A similar trend was observed in the Marine collagen group, where the half-dose with GI reached a peak of about 10% compared to control ($p < 0.05$), outperforming the full-dose treatment ($p < 0.05$). However, the biomimetic formulation (Figure 5E) was associated with the largest increase among the tested conditions; indeed, the GI enhanced half-dose reached a peak improvement of about 32% compared to control ($p < 0.05$), significantly exceeding the 25% observed for the full-dose combination ($p < 0.05$) and maintaining a 14% lead over the SH ($p < 0.05$). A similar dose-dependent trend was observed in Zo-1 expression levels (Figure 5B,D,F), which are critical for the architectural stability of the barrier. In the Marine collagen group (Figure 5B), the full dose combined with GI peaked at 19% compared to control ($p < 0.05$), while the half-dose stabilised at a slightly lower but highly efficient 16% ($p < 0.05$). In contrast, the Bovine collagen group (Figure 5D) showed a clear preference for the reduced dosage, with the GI-boosted half-dose eliciting a peak increase of 25% compared to control ($p < 0.05$), versus the 21% achieved by the full-dose combination ($p < 0.05$). Furthermore, in the biomimetic formulation group (Figure 5F), the GI-enhanced half-dose achieved the greatest upregulation across the study, at nearly 30% compared to control ($p < 0.05$), whereas the full-dose combination reached approximately 22% ($p < 0.05$). Collectively, these molecular findings suggested that while all tested preparations increased the measured tight-junction protein levels, the half-dose integration of GI was associated with the highest increase in tight-junction-related markers among the conditions tested.

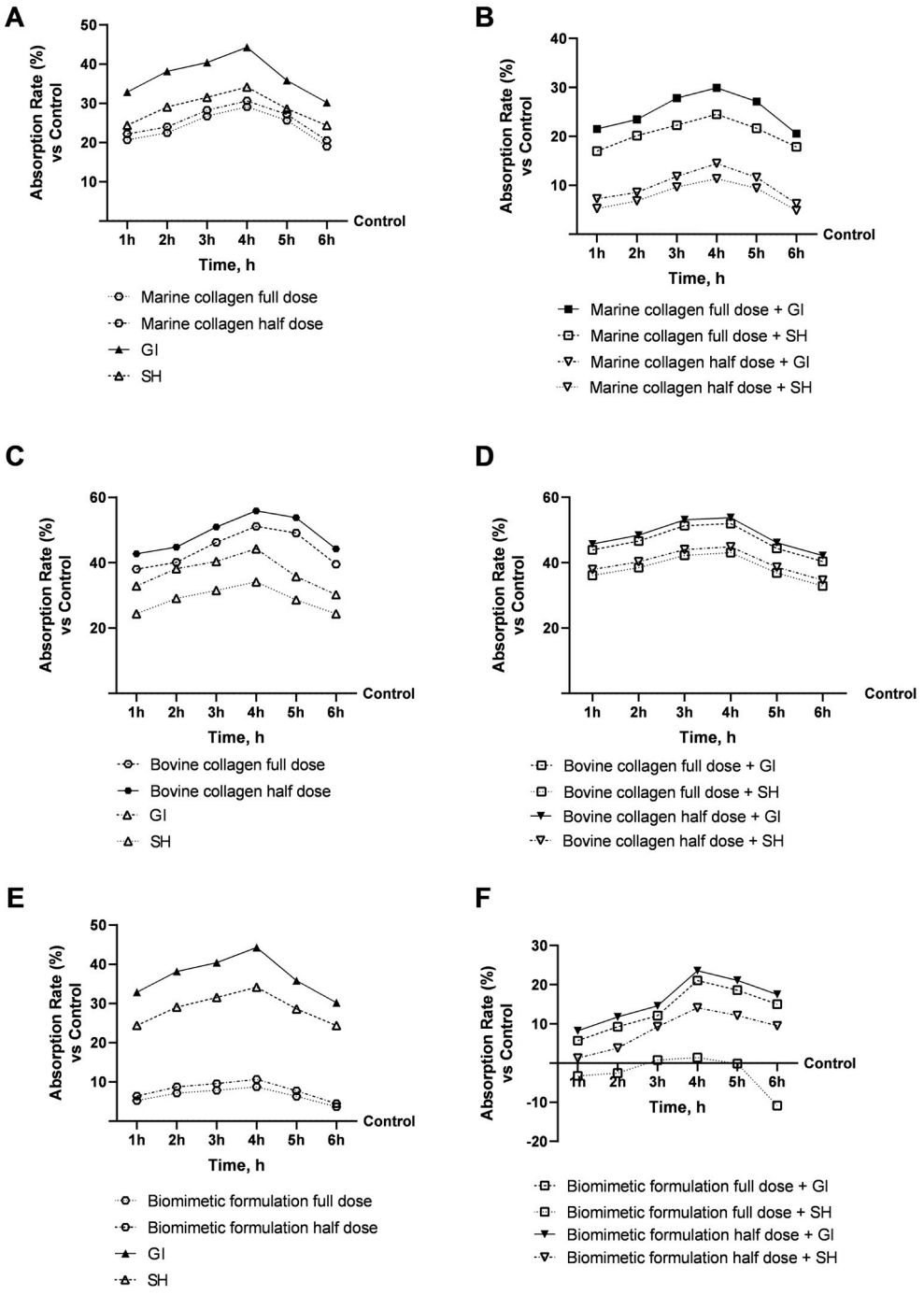


Figure 3. Assessment of intestinal permeability in the Caco-2 Transwell system. In (**A**,**C**,**E**), permeability (%) is reported for the individual preparations (marine and bovine collagen hydrolysates and the biomimetic formulation, at full and half doses) and for GI and SH. In (**B**,**D**,**F**), the permeability analysis of the respective combinations of the three preparations with GI or SH over a 6 h period was reported. The abbreviations are the same as reported in Figure 1. The baseline (0%) represents the control values. Results are expressed as mean ± SD (%) of five independent experiments conducted in triplicate.

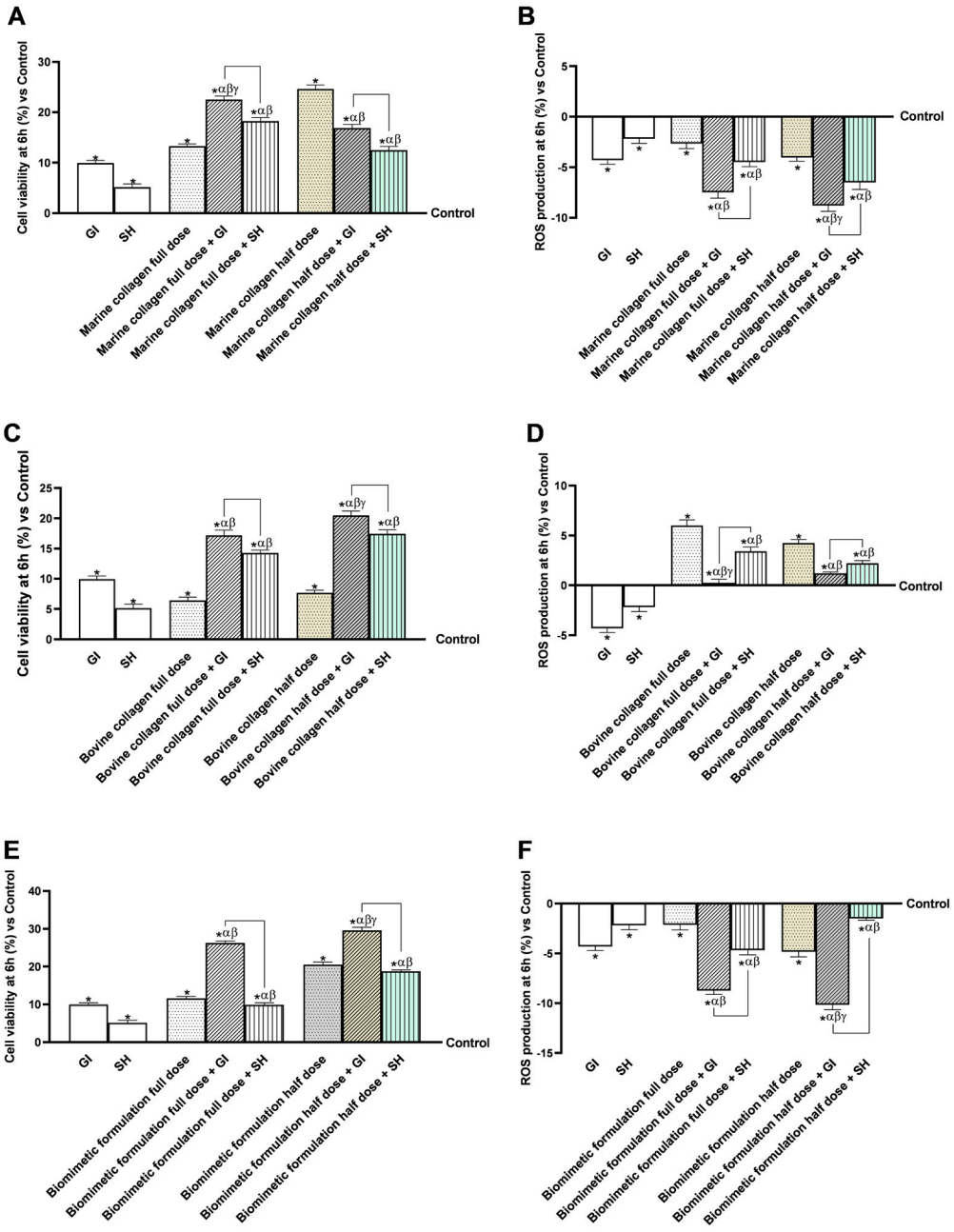


Figure 4. Cell viability and intracellular ROS production in Caco-2 cells. In (**A**,**C**,**E**), cell viability (%) is reported for the individual preparations (marine and bovine collagen hydrolysates and the biomimetic formulation, at full and half doses) and for GI and SH. In (**B**,**D**,**F**), ROS production (%) of the respective combinations of the three preparations with GI or SH over a 6 h period was reported. The abbreviations are the same as reported in Figure 1. The results are expressed as mean ± SD (%) of five independent experiments normalised to the control (0 line corresponding to 100% cell viability), each performed in triplicate and expressed as the percentage increase. * $p < 0.05$ vs. control; α $p < 0.05$ vs. GI and SH; β $p < 0.05$ vs. collagen full and half dose; the bar indicates $p < 0.05$ vs. collagen + SH; γ $p < 0.05$ vs. all formulation tested.

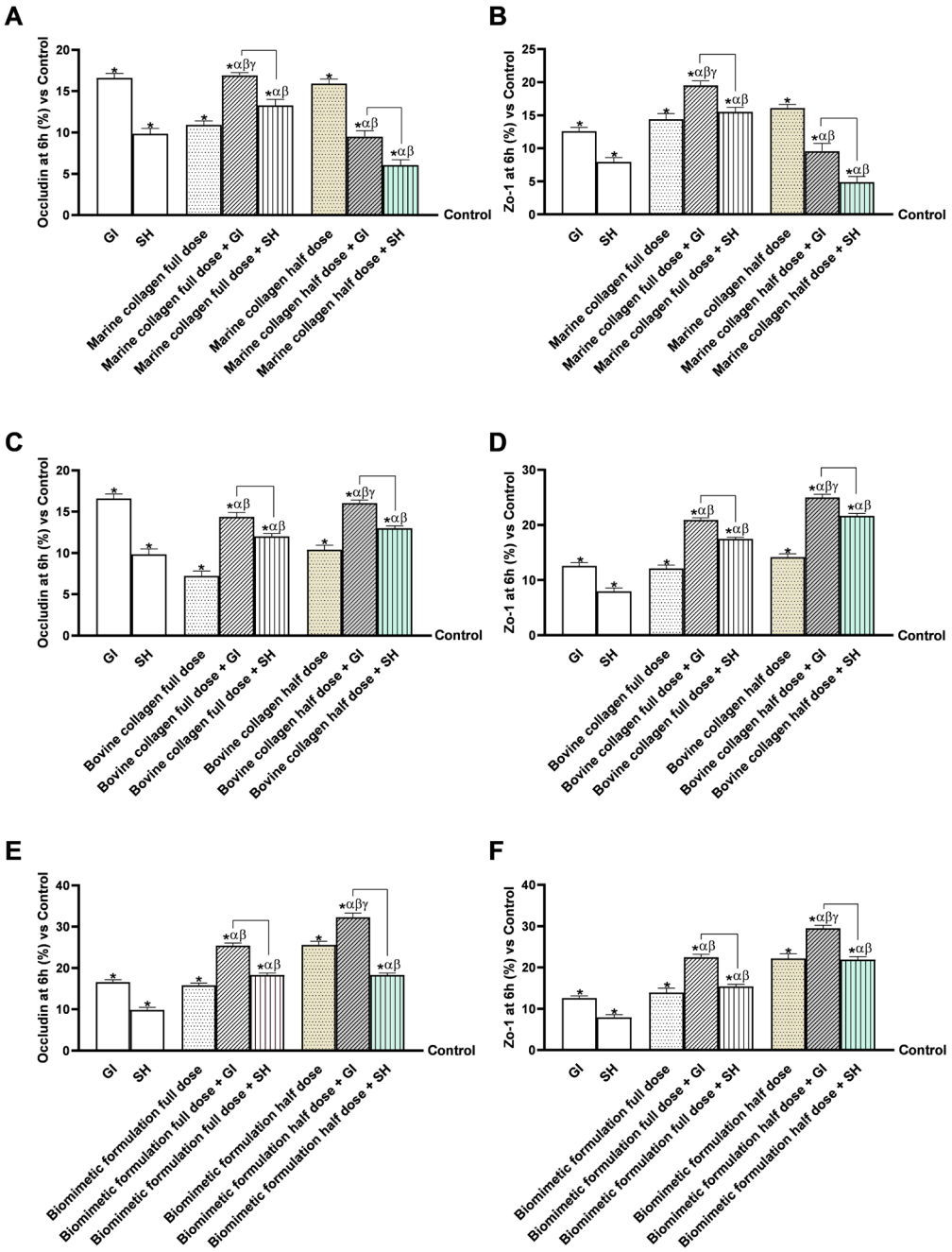


Figure 5. Molecular analysis of TJ protein levels by ELISA Kit. In (**A**,**C**,**E**), the relative expression (%) of Occludin is reported for the individual preparations (marine and bovine collagen hydrolysates and the biomimetic formulation, at full and half doses) and for GI and SH. In (**B**,**D**,**F**), the relative expression (%) of Zo-1 of the respective combinations of the three preparations with GI or SH was reported. The abbreviations are the same as reported in Figure 1. Data are expressed as mean ± SD (%) of 5 independent experiments performed in triplicate vs. control * $p < 0.05$ vs. control; α $p < 0.05$ vs. GI and SH; β $p < 0.05$ vs. collagen full and half dose; the bar indicates $p < 0.05$ vs. collagen + SH; γ $p < 0.05$ vs. all formulation tested.

3.3. Effects of Basolateral Medium on Cellular and Extracellular Matrix Responses in the Skin Co-Culture Model

Responses in the skin co-culture model were evaluated following 24-h exposure to basolateral medium collected from Caco-2 cultures after 6 h of treatment with the tested preparations. Under the experimental conditions tested, no cytotoxic effects were observed for any treatment. Differences were observed between the two hyaluronic acid deriva-

tives: GI was generally associated with greater increases in metabolic activity and elastin production than SH under the experimental conditions tested ($p < 0.05$). Analysis of the viability data (Figure 6A–C) indicated that GI was associated with greater modulation of cellular responses under the experimental conditions tested. In the Marine collagen group (Figure 6A), the integration of GI resulted in a viability peak of approximately 12% compared to the control ($p < 0.05$), nearly doubling the 7% achieved by the SH combination ($p < 0.05$). A consistent dose-dependent trend also emerged: the half-dose combinations frequently outperformed the full-dose applications ($p < 0.05$). These findings suggest that lower concentrations may be sufficient to elicit measurable cellular responses in this experimental model, as seen in the Bovine collagen group (Figure 6B), where the GI half-dose reached a peak of 20% compared to control ($p < 0.05$), maintaining a clear lead over the 17% recorded for its SH counterpart ($p < 0.05$).

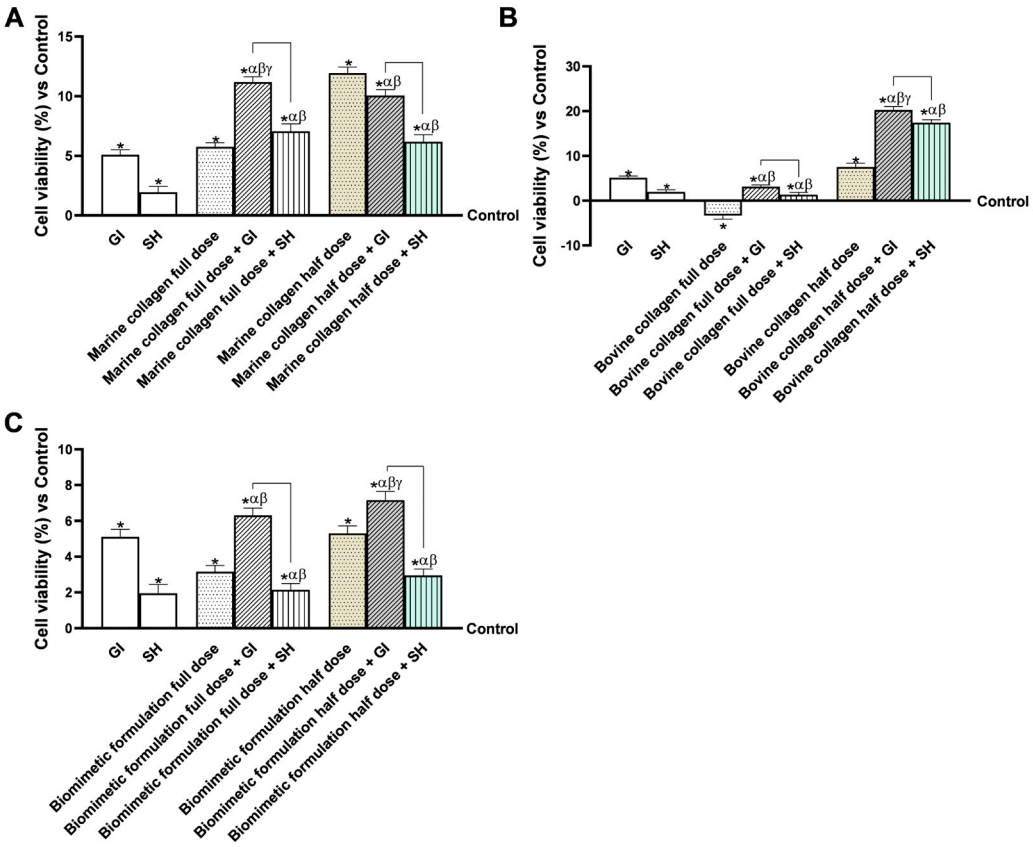


Figure 6. Cell viability in the skin co-culture model. In (**A**–**C**), cell viability (%) is reported for the individual preparations (marine and bovine collagen hydrolysates and the biomimetic formulation, at full and half doses) and for GI and SH. The abbreviations are the same as reported in Figure 1. Data are expressed as mean ± SD (%) of 5 independent experiments performed in triplicate vs. control * $p < 0.05$ vs. control; α $p < 0.05$ vs. GI and SH; β $p < 0.05$ vs. collagen full and half dose; the bar indicates $p < 0.05$ vs. collagen + SH; γ $p < 0.05$ vs. all formulations tested.

To further characterise extracellular matrix-related responses, type I collagen levels and COL1A1 protein expression were analysed. These results indicate that the tested combinations modulated markers associated with extracellular matrix organisation. As observed in the previous metabolic assays, GI was generally associated with higher collagen-related responses than the SH variant under the experimental conditions tested ($p < 0.05$), with half-dose combinations frequently associated with greater increases in collagen-related measurements. Analysis of Type I Collagen expression (Figure 7A,C,E) revealed a significant upregulation across all treatment groups. In the Marine collagen series (Figure 7A),

the integration of GI at a full dose stimulated an about 6.8% increase compared to control ($p < 0.05$), whereas the SH combination achieved only about 5.5% compared to control ($p < 0.05$). However, the most striking results were observed with the Biomimetic formulation (Figure 7E); here, the GI-enhanced half-dose was associated with an approximately 20% increase in measured type I collagen levels compared to control ($p < 0.05$), representing a substantial about 6% lead over the alternative hyaluronic acid combination (about 14% vs. control, $p < 0.05$) and significantly outperforming the full-dose application ($p < 0.05$). Similarly, in the Bovine collagen group (Figure 7C), the GI half-dose integration increased by about 7.2% compared to the control ($p < 0.05$), nearly doubling the stimulus provided by collagen alone (about 5%, $p < 0.05$). Analysis of COL1A1 protein expression (Figure 7B,D,F) showed a consistent trend towards higher levels with GI-containing combinations than with the corresponding SH-containing combinations. In the Bovine collagen group (Figure 7D), the combination with GI at half-dose elicited an approximately 6.8% increase compared to the control ($p < 0.05$), outperforming the SH variant. The Biomimetic group (Figure 7F) showed the largest response among the tested conditions, with the half-dose combination containing GI showing an approximately 19.2% increase in COL1A1 protein expression relative to control ($p < 0.05$), whereas the SH counterpart remained below about 13.2% relative to control ($p < 0.05$). Notably, half-dose conditions were frequently associated with larger responses than the corresponding full-dose regimens ($p < 0.05$), though the full-dose regimens occasionally showed diminishing returns. These findings suggest that GI, particularly when combined with selected concentrations of the tested preparations, was associated with increased expression of extracellular matrix homeostasis markers under the experimental conditions tested.

Further characterisation of the skin co-culture model included measurement of type III and type IV collagen levels (%). Consistent with data from other structural markers, integration with GI exhibited markedly higher biological activity than the SH variant ($p < 0.05$), with GI-containing combinations generally showing larger responses than the corresponding SH-containing conditions. Firstly, the data for Type III Collagen (Figure 8A,C,E), which is essential for tissue elasticity and the initial repair phases, show a consistent trend toward a stronger biological response for the GI derivative. In the Bovine collagen group (Figure 8C), the combination with GI at half-dose elicited an approximately 5.5% increase compared to the control ($p < 0.05$), outperforming the SH variant. The Biomimetic group (Figure 8E) again demonstrated the highest overall biological activity, with the half-dose combination containing GI showing an approximately 11% increase in measured type III collagen levels relative to control ($p < 0.05$), whereas the SH counterpart remained below about 7% of control ($p < 0.05$). Notably, the half-dose strategies consistently yielded a more robust and statistically significant stimulus ($p < 0.05$) than the full-dose regimens, which occasionally showed diminishing returns. These findings suggest that GI, particularly when paired with selected concentrations of the tested preparations, was associated with greater induction of key structural protein markers under the experimental conditions tested. Analysis of type IV collagen levels (Figure 8B,D,F) showed generally higher measured levels with GI-containing combinations than with the corresponding SH-containing combinations under the experimental conditions tested. In the Biomimetic formulation group (Figure 8F), the half-dose combination containing GI was associated with an increase of nearly 6% in measured type IV collagen levels relative to control, significantly outperforming both its full-dose counterpart and the combination with the alternative HA (about 4%). A similar trend is visible in the Bovine collagen group (Figure 8D), where the half-dose with GI nearly quintupled the effect of collagen alone, reaching a peak of over 4.5% compared to the SH variant's 3.3%. Again, the half-dose proved to be the more efficient strategy for maximising protein expression.

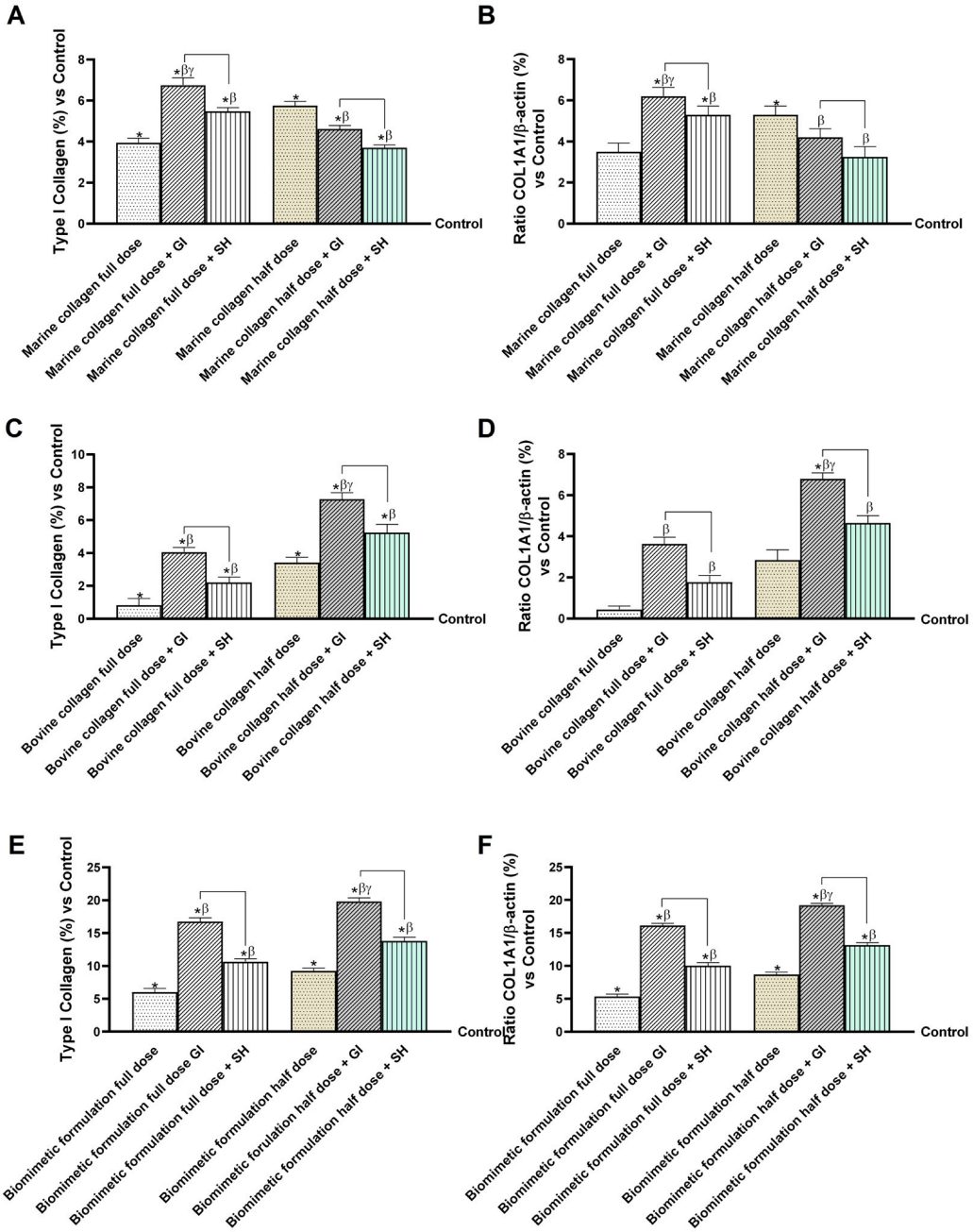


Figure 7. Type I collagen levels and COL1A1 protein expression in the skin co-culture model. In (**A**,**C**,**E**), relative type I collagen levels (%) are reported for the bovine and marine collagen hydrolysates and the biomimetic formulation, at full and half doses, alone or in combination with GI or SH. In (**B**,**D**,**F**), COL1A1 protein expression is reported for the three preparations, at full and half doses, alone or in combination with GI or SH. The abbreviations are the same as reported in Figure 1. Representative COL1A1 gel lanes for each of the three preparations are provided in the Appendix, Figures A2–A4 (panel B). Data are expressed as mean ± SD (% relative to control) from five independent experiments for the collagen assay (panels A, C and E) and three independent experiments for COL1A1 Western blot analysis (panels B, D and F), each performed in technical triplicate; * $p < 0.05$ vs. control; β $p < 0.05$ vs. collagen full and half dose; the bar indicates $p < 0.05$ vs. collagen + SH; γ $p < 0.05$ vs. all formulation tested.

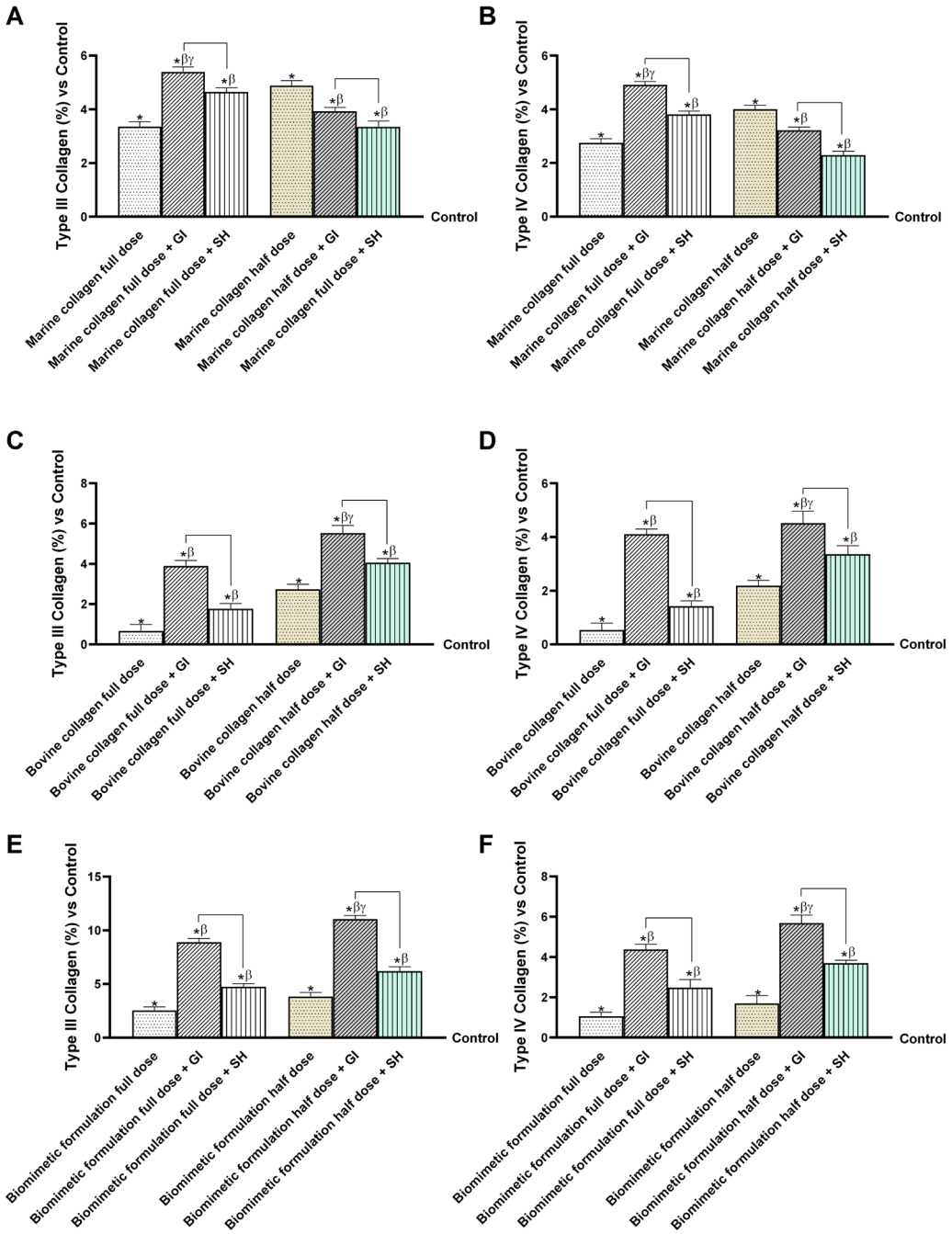


Figure 8. Type III and type IV collagen levels in the skin co-culture model. In (**A**,**C**,**E**), relative type III collagen levels (%) are reported for the bovine and marine collagen hydrolysates and the biomimetic formulation, at full and half doses, alone or in combination with GI or SH. In (**B**,**D**,**F**), relative type IV collagen levels (%) are reported for the three preparations, at full and half doses, alone or in combination with GI or SH. The abbreviations are the same as reported in Figure 1. Data are expressed as mean ± SD (%) of 5 independent experiments performed in triplicate vs. control; * $p < 0.05$ vs. control; β $p < 0.05$ vs. collagen full and half dose; the bar indicates $p < 0.05$ vs. collagen + SH; γ $p < 0.05$ vs. all formulations tested.

In conclusion, these results demonstrate that the addition of GI enhances the action of all tested preparations to a greater extent than the SH variant ($p < 0.05$). Overall, GI-containing combinations were generally associated with greater modulation of collagen-related markers than the corresponding SH-containing conditions. This pattern was observed for both fibrillar collagens (types I and III) and type IV collagen, with several of the largest responses occurring at the half-dose concentration of the tested preparations.

These findings support further investigation of the interaction between preparation type, preparation concentration, and HA formulation in the regulation of ECM-related responses.

3.4. Effects on Hyaluronic Acid Levels and ECM-Related Markers

To further investigate the molecular pathways underlying extracellular matrix (ECM) modulation, Western blot analyses were conducted on skin co-culture model lysates following exposure to basolateral medium collected from treated Caco-2 cultures. Four key biomarkers involved in skin ECM homeostasis and remodelling were evaluated: HA content; ELN, a structural protein essential for skin elasticity and resilience; HAS2, the primary enzyme responsible for HA biosynthesis; and MMP1, a collagen-degrading enzyme associated with ECM breakdown and skin ageing. Together, these markers provide information on molecular responses associated with ECM homeostasis and remodelling in the skin co-culture model.

Initially, HA content was measured in the skin co-culture model. Figure 9A,C,E show changes in HA content following exposure to the different treatments. GI-containing combinations generally showed greater modulation of HA content than the corresponding SH-containing conditions: in the biomimetic formulation group (Figure 9E), the half-dose combination with GI was associated with an approximately 45% increase in HA content relative to control, compared with approximately 37% for the corresponding SH-containing combination. Notably, in the Bovine collagen group (Figure 9C), the addition of GI transformed the nearly negligible or negative baseline effect of collagen alone into a net, statistically relevant increase. Overall, combinations of the tested preparations with GI were associated with greater increases in HA content than the corresponding SH-containing combinations ($p < 0.05$).

A similar trend was observed for ELN expression. As shown in Figure 9B,D,F, GI-containing combinations were associated with changes in ELN protein expression, a marker related to ECM homeostasis. While the individual preparations showed limited activity, their combination with GI resulted in a significant increase compared with the control ($p < 0.05$). The strongest effect was observed in the biomimetic formulation group (Figure 9F), where the GI half-dose achieved the largest increase in elastin in the study (26% vs. control, $p < 0.05$), exceeding the SH formulation (15% vs. control, $p < 0.05$) by 11%. Notably, half-dose combinations consistently outperformed full-dose treatments, which, in the case of Bovine collagen (Figure 9D), showed slightly negative effects when administered alone. Collectively, these findings indicate that GI-containing combinations, particularly at the half-dose concentrations of the collagen hydrolysates and the biomimetic formulation, were associated with greater modulation of ECM-related parameters under the experimental conditions tested. The quantitative comparison presented in Appendix B (Tables A2–A4) corroborates the general trend towards greater modulation of ECM-associated markers in formulations containing GI compared to the corresponding conditions containing SH.

Among the tested formulations, biomimetic formulation combined with GI exhibited one of the most pronounced modulation profiles, characterised by increased expression of ECM-related proteins and reduced or stable MMP1 levels. In selected GI-containing combinations, increased HAS2 expression was accompanied by reduced or stable MMP1 levels. Although these molecular alterations do not constitute direct evidence of tissue regeneration, they may indicate changes in molecular pathways associated with extracellular matrix homeostasis. The coordinated modulation of COL1A1, HAS2, ELN, and MMP1 should therefore be interpreted as evidence of extracellular matrix-related molecular responses under the experimental conditions examined, rather than as direct proof of tissue repair or regeneration processes.

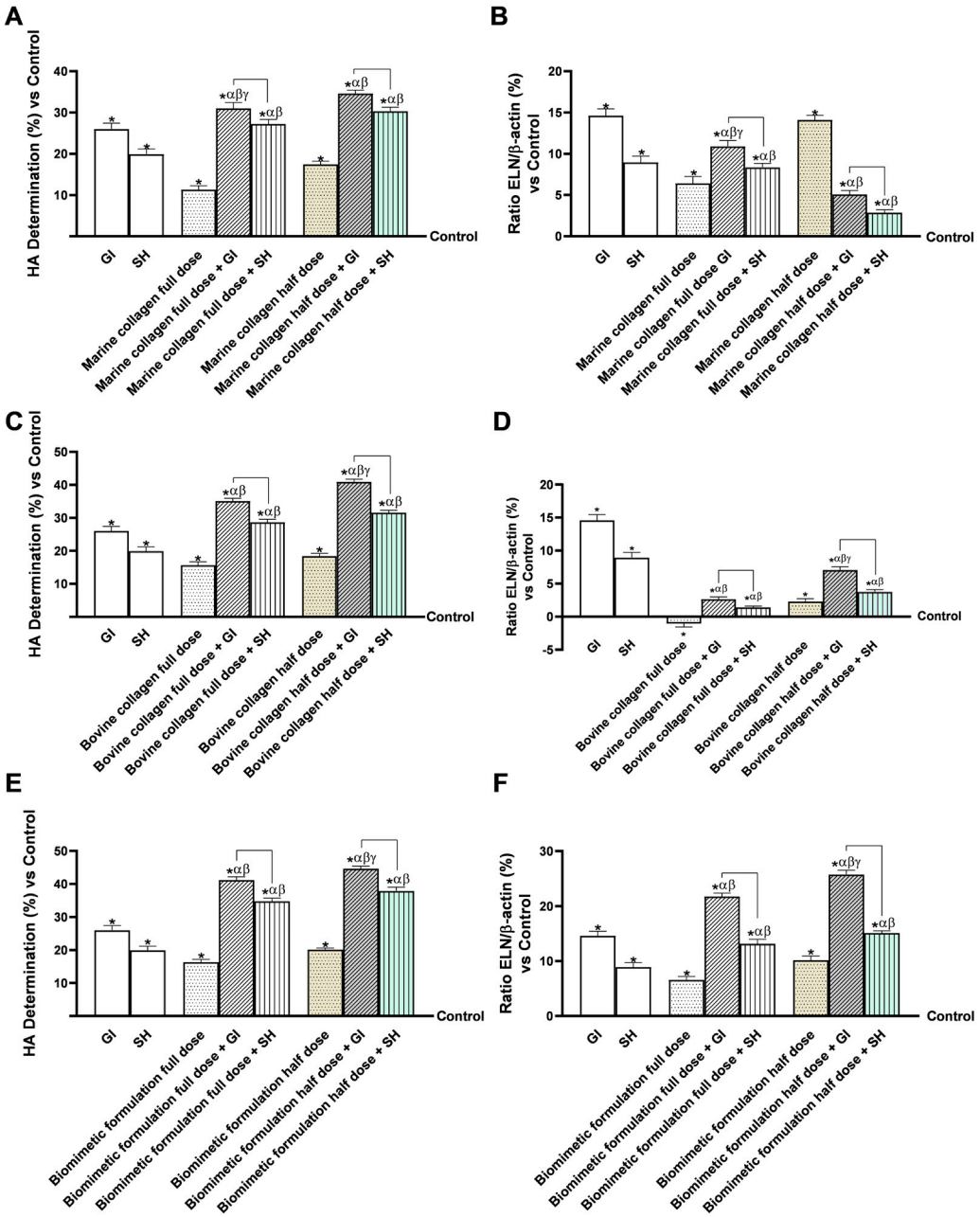


Figure 9. HA content and ELN protein expression in the skin co-culture model. In (**A**,**C**,**E**), the relative quantification (%) of HA content from individual preparations (Marine collagen, Bovine collagen, and biomimetic formulation at full and half doses) and from GI and SH was reported. In (**B**,**D**,**F**), the relative expression (%) of ELN of the respective combinations of three preparations with GI or SH was reported. The abbreviations are the same as reported in Figure 1. Representative ELN gel lanes for each preparation are provided in the Appendix, Figures A2–A4 (panel F). Data are expressed as mean ± SD (% relative to control) from five independent experiments for the HA assay (panels A, C and E) and three independent experiments for ELN Western blot analysis (panels B, D and F), each performed in technical triplicate; * $p < 0.05$ vs. control; α $p < 0.05$ vs. GI and SH; β $p < 0.05$ vs. collagen full and half dose; the bar indicates $p < 0.05$ vs. collagen + SH; γ $p < 0.05$ vs. all formulation tested.

The data related to HAS2 expression were reported in Figure 10A,C,E and it was revealed that GI showed a greater biological activity: in the Bovine collagen model (Figure 10C), the half-dose combination with GI induced a major expression of HAS2 of about 40% compared to the combination with the alternative HA (about 30%). More-

over, the most significant enhancement was observed in the Biomimetic preparation group (Figure 10E), where the GI-boosted half dose increased HAS2 expression the most, with a value of approximately 43% relative to the control ($p < 0.05$), outperforming the SH variant by approximately 8% ($p < 0.05$).

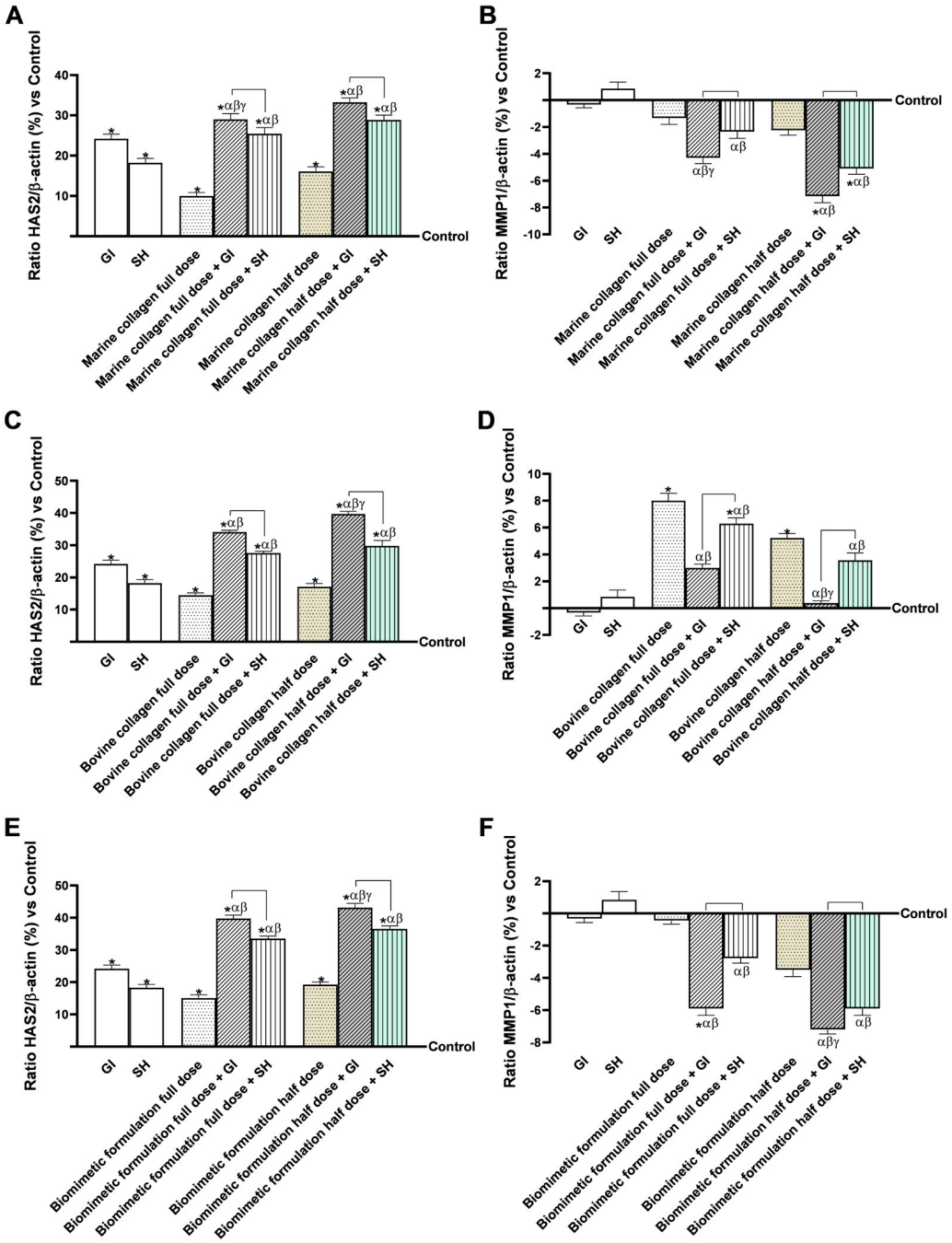


Figure 10. HAS2 and MMP1 protein expression in the skin co-culture model. In (**A**,**C**,**E**), the expression (%) of HAS2 of individual preparations (Marine collagen, Bovine collagen, and biomimetic formulation at full and half doses) and of GI and SH were reported. In (**B**,**D**,**F**), the expression (%) of MMP1 of the respective combinations of three preparations with GI or SH was reported. The abbreviations are the same as reported in Figure 1. Representative HAS2 and MMP1 gel lanes for each preparation are provided in the Appendix, Figures A2–A4 (panel F). Data are expressed as mean ± SD (% relative to control) from three independent experiments, each performed in technical triplicate; * $p < 0.05$ vs. control; α $p < 0.05$ vs. GI and SH; β $p < 0.05$ vs. collagen full and half dose; the bar indicates $p < 0.05$ vs. collagen + SH; γ $p < 0.05$ vs. all formulations tested.

An opposite trend was observed in MMP1 expression results (Figure 10B,D,F). Indeed, the data for MMP1 further underscore the functionally stronger biological response of GI over other forms of HA. Combinations of the tested preparations with GI were associated with changes in MMP1 expression compared with the control ($p < 0.05$), suggesting modulation of pathways involved in ECM turnover. The largest reduction was observed in the Biomimetic formulation group (Figure 10F), where the GI-enhanced half-dose resulted in MMP1 levels approximately 7.2% below the control ($p < 0.05$), with a greater reduction than that observed for the corresponding SH-containing condition ($p < 0.05$). Furthermore, the data show that half-dose combinations consistently provide a more balanced and effective stimulus than full doses, which, in some cases (Figure 10B,D), showed slightly negative effects when administered alone. In conclusion, these results confirm that the inclusion of GI, particularly at an optimised half-dose, was associated with the most favourable balance between HAS2 and MMP1 modulation among the conditions tested.

Collectively, these results indicate that the observed shift towards enhanced HAS2 expression and reduced MMP1 levels is consistent with the modulation of molecular pathways associated with extracellular matrix homeostasis and hyaluronic acid biosynthesis in GI-containing formulations.

4. Discussion

Skin ageing and connective tissue degeneration represent increasingly relevant health concerns in modern societies, driven by both intrinsic biological processes and environmental factors such as oxidative stress, UV exposure, and lifestyle habits. ECM plays a significant role in maintaining structure, elasticity, and function within this context [41]. Collagen and HA, two of the most abundant ECM components, have attracted considerable attention as nutraceutical agents because they can modulate tissue homeostasis. Despite their growing interest, the mechanisms underlying their combined biological activity, particularly after oral administration, remain incompletely understood [42].

In this context, we evaluated the biological activity of different collagen–HA combinations, assessing their biological activity at the intestinal level and in skin cells to provide a more comprehensive understanding of their potential effects along the gut–skin interaction. Additional hyaluronan and hydroxyproline measurements provided further biochemical characterisation of the material recovered in the basolateral compartment. However, these measurements do not establish the molecular identity, molecular-weight distribution, structural integrity or biological activity of the recovered components. Therefore, they should be interpreted as analytical markers of recovered material rather than as evidence of specific transported molecular species. The intestinal barrier is the first interface for orally administered compounds. Preservation of intestinal epithelial integrity, together with the modulation of TJ proteins such as ZO-1 and occludin, indicates that collagen-based formulations help to maintain barrier function under the experimental conditions tested. In our study, increased TEER values and upregulation of TJ components further support this effect. These findings are consistent with previous studies indicating that collagen-derived peptides can support epithelial homeostasis and barrier function by modulating intercellular junctions and reducing permeability [43,44]. The combination with HA was generally associated with stronger modulation of these parameters, suggesting a cooperative interaction at the intestinal level. Among the tested HA formulations, GI-containing formulations generally showed stronger effects than SH-containing formulations under the experimental conditions tested, indicating that molecular characteristics such as structure, molecular weight, or bioavailability may contribute to differences in biological activity [45]. Interestingly, a clear dose-dependent trend emerged throughout the study, as half-dose formulations frequently outperformed full-dose treatments. This suggests that the best

biological responses may occur at lower concentrations, possibly due to receptor saturation or feedback regulatory mechanisms. Similar results have been observed in studies of bioactive peptides and ECM-related signalling pathways, in which high concentrations may attenuate cellular responsiveness. These observations may be relevant for the optimisation of collagen- and HA-based nutraceutical formulations [46,47]. In addition to protecting the barrier function, the tested compounds significantly improved intestinal permeability. The observed increase in transepithelial passage indicates that HA-containing formulations may have an effect on the dynamics of transport across the epithelial model. The potential mechanisms may involve modulation of barrier-related pathways, although these were not directly investigated in the present study, as previously reported [48]. The observed effects on permeability suggest that HA-containing combinations may modulate intestinal transport dynamics in vitro. The transport results were further corroborated by the direct quantification of hyaluronic acid and collagen recovered in the basolateral compartment, confirming the presence of material attributable to the compound following passage through the intestinal barrier model. However, it is important to note that these observations should be interpreted as evidence of transport across an in vitro epithelial model, rather than as a direct measure of systemic bioavailability or in vivo intestinal metabolism. Additional hyaluronan and hydroxyproline measurements provided further biochemical characterisation of the recovered material. Another key aspect investigated in this study is oxidative stress, because it plays a significant role in the development of intestinal dysfunctions and ageing. Our results demonstrated that all treatments exerted antioxidant effects, reducing ROS production in intestinal cells. This protective activity was significantly enhanced with combination treatments, particularly those including GI. These findings are in line with previous studies highlighting the antioxidant properties of both collagen peptides and HA and suggest the involvement of cellular pathways associated with oxidative balance and cellular defence mechanisms [49,50].

In the second phase of this study, the focus was on the effects of basolateral medium collected from treated Caco-2 cultures on a skin co-culture model in order to evaluate the gut–skin interaction. This approach allowed us to evaluate the biological impact of basolateral medium collected from treated Caco-2 cultures on cells in the skin co-culture model, providing a more physiologically relevant perspective than conventional single-cell models [51]. All treatments were associated with maintained or increased cell viability in the skin co-culture model, as assessed by the MTT assay, supporting the absence of detectable cytotoxic effects under the experimental conditions tested. The treatments were associated with increased measured levels of ECM components, including collagen types I, III and IV, elastin and HA. These findings are highly relevant to skin physiology. Type I collagen is the primary structural protein of the dermis, while type III collagen is associated with tissue repair and early remodelling processes. Type IV collagen, on the other hand, is an important component of the basement membrane and plays a crucial role in maintaining epidermal–dermal cohesion [52,53]. Taken together, these results suggest that the tested formulations may modulate multiple signalling pathways related to the extracellular matrix and associated with skin homeostasis, acting on various structural components of the skin.

In line with intestinal findings, the combination treatments, particularly those including GI, generally showed stronger modulation of ECM synthesis [54,55]. These results suggested that collagen and HA may contribute to reproducing an extracellular matrix-related signalling condition to promote cellular activity. Although biomimetic formulation generally showed larger responses, the magnitude of the differences varied across endpoints and should be interpreted cautiously because the formulations differ in composition and physicochemical characteristics. The biomimetic preparation differs compositionally from the bovine and marine collagen hydrolysates, as it comprises selected amino acids, vitamin

C, Centella asiatica extract and Panax ginseng extract. The responses observed with this preparation therefore reflect the activity of the complete formulation. As its constituents were not tested separately, their individual contributions to the observed effects cannot be determined. The observed modulation of elastin levels further supports the involvement of extracellular matrix-related pathways, as elastin is a key structural component contributing to tissue elasticity and resilience [55]. A noteworthy finding is the increased HA content in the skin co-culture model, which, together with increased HAS2 expression, is consistent with a possible stimulation of HA biosynthesis [56]. These findings suggest that the treatments may influence not only extracellular matrix composition, but also cellular pathways associated with endogenous HA homeostasis [56]. These findings suggest a potential contribution to molecular processes involved in tissue maintenance. As observed in the intestinal study, half-dose combinations frequently produced larger responses than the corresponding full-dose conditions. These findings suggest that lower concentrations may provide more favourable biological modulation under the tested experimental conditions, likely due to improved signalling dynamics and a reduced risk of negative feedback effects. These observations may support future investigations into collagen- and HA-based nutraceutical approaches targeting skin physiology [57].

Despite these promising findings, several limitations should be acknowledged. First, although the gut–skin interaction model used in this study represents an advanced in vitro system, it cannot fully replicate the complexity of human physiology. In particular, interactions with the immune, endocrine, and nervous systems are not accounted for and may influence the in vivo response. Second, although the skin co-culture model incorporates primary human cells, it cannot reproduce inter-individual variability or the full cellular complexity of human intestinal and skin tissues. Third, the study focused on short-term exposure, and therefore, long-term effects, cumulative responses, and potential adaptive mechanisms were not evaluated. Moreover, hydroxyproline analysis provided additional compositional information but does not establish collagen structure, peptide sequence or molecular integrity. Nevertheless, the integrated gut–skin approach adopted in the present study was designed to reproduce selected aspects of the physiological gut-skin–axis, a bidirectional communication network which has been increasingly recognised as a factor in skin homeostasis through intestinal-derived nutrients, metabolites, and signalling molecules. The combination of a differentiated Caco-2 intestinal barrier with a skin co-culture model provides a physiologically relevant platform for evaluating biological responses following intestinal passage. Further analyses of hyaluronan and hydroxyproline in the basolateral compartment provided further biochemical characterisation of the recovered material. However, it should be noted that these measurements do not establish the molecular identity, molecular-weight distribution, structural integrity, or biological activity of the recovered components. Therefore, they should be interpreted as analytical markers of recovered material rather than direct evidence of specific transported molecular species. Additionally, while the transfer experiments demonstrate that basolateral medium obtained from treated intestinal cultures can modulate several skin-cell endpoints, the present experimental design does not allow attribution of these responses exclusively to transported collagen- or hyaluronic acid-derived material. The observed biological effects may also be attributed to treatment-induced factors released by Caco-2 cells. Consequently, the skin co-culture responses should be interpreted as the result of exposure to conditioned basolateral medium generated by treated intestinal cultures, rather than as direct evidence of the activity of a specific transported molecular species.

However, the model does not fully reproduce the complexity of the in vivo gut–skin axis, as it lacks systemic circulation, liver metabolism, microbiota-host interactions, immune responses, and neuroendocrine regulation. Consequently, the findings should be

interpreted as evidence derived from a controlled in vitro model of gut–skin interaction rather than as a complete representation of human physiological conditions. While the present model provides biologically relevant information on gut–skin interactions, further in vivo and clinical investigations will be required to confirm the physiological relevance of the observed responses in humans. Furthermore, while significant modulation of key ECM markers and oxidative stress parameters was observed, deeper mechanistic insights were not explored and should be addressed in future studies. Moreover, while the concentrations utilised in this study were selected based on extant literature and preliminary dose–response experiments, they should be interpreted as experimental concentrations suitable for investigating biological responses under controlled in vitro conditions. In order to extrapolate these results to human exposure conditions following oral administration, an appropriate pharmacokinetic assessment and translational approaches are required.

The additional Western blot analyses further supported these observations, showing modulation of proteins directly involved in extracellular matrix synthesis and remodelling, including COL1A1, HAS2, ELN, and MMP1. In particular, the concurrent increase in HAS2 expression and reduction or stability of MMP1 levels in selected GI-containing combinations suggests modulation of pathways involved in HA biosynthesis and collagen turnover, consistent with a potential role in ECM homeostasis. These findings provide additional mechanistic support for the extracellular matrix-related effects observed in the functional assays. Finally, although the data strongly support the potential combined biological effects of collagen–HA combinations, clinical validation remains essential to confirm their biological activity and safety in human populations.

5. Conclusions

In conclusion, the present study suggests that combinations of bovine and marine collagen hydrolysates and a compositionally distinct biomimetic formulation, together with distinct hyaluronic acid formulations, may modulate extracellular matrix-related pathways within an integrated gut–skin in vitro model. The tested formulations were associated with the maintenance of intestinal barrier integrity, modulation of tight junction-related proteins, and increased measured levels of extracellular matrix components, including collagens, elastin, and hyaluronic acid, following simulated intestinal passage.

Additional Western blot analyses further supported the modulation of ECM-related proteins, including COL1A1, HAS2, ELN, and MMP1, suggesting changes in molecular pathways associated with extracellular matrix homeostasis in selected combinations. Consequently, the observed modulation of ECM-related markers should be interpreted as evidence of alterations in molecular pathways associated with ECM homeostasis, rather than as direct evidence of tissue regeneration or repair.

Overall, these findings provide preliminary mechanistic evidence supporting the potential relevance of collagen- and hyaluronic acid-based formulations in extracellular matrix homeostasis and gut–skin interaction signalling under the tested experimental conditions.

While the present results provide biologically relevant information within a controlled in vitro model, further in vivo and clinical studies will be required to confirm the physiological relevance, translational potential, and biological mechanisms underlying the effects observed in humans.

Supplementary Materials: The following supporting information can be downloaded at: https://www.mdpi.com/article/10.3390/cosmetics13060295/s1, **Figure S1**. Representative Tricine-SDS-PAGE analysis of the collagen-derived formulation under investigation. L1: molecular weight marker; L2: biomimetic formulation; L3: bovine collagen; L4: marine collagen. The samples were separated on 16% Tricine-SDS polyacrylamide gels and stained with Coomassie Brilliant Blue R-250. The bovine and marine collagen showed diffuse staining primarily in the gel region corresponding to 2 kDa, consistent with hydrolyzed collagen peptide preparations. The biomimetic formulation displayed an electrophoretic profile similar to that of the other two collagens. Under the analytical conditions employed, the electrophoretic profiles provide qualitative information regarding peptide distribution and allow for the differentiation of the tested materials, but they do not constitute a quantitative determination of the average molecular weight or the molecular weight distribution; **Figure S2**. Agarose gel electrophoresis analysis of hyaluronic acid preparations. L1: molecular weight standards (Select-HA HiLadder and Select-HA Mega Ladder) covering an approximate molecular weight range of 500–4000 kDa. L2: sodium hyaluronate preparation (1 mg/mL). L3: GreenIuronic® preparation YET250224W28-01 (1 mg/mL). Molecular weight determination was performed as described in Supplementary Method S4; **Table S1**. The values are reported as the mean ± standard deviation from three independent preparations. The hydroxyproline content of bovine collagen, marine collagen and the biomimetic formulation is reported in Table 1 of the main manuscript and is therefore not repeated here; **Table S2**. The values are reported on the basis of confirmatory analyses of the certificates of analysis and manufacturers' technical documentation regarding the batches used in this study. The molecular weight analysis of the gel is presented below.

Author Contributions: Conceptualization, F.P. and F.U.; methodology, F.P., M.M., S.M. and R.G.; software, F.P., M.M., S.M. and R.G.; validation, M.M., S.M. and F.U.; formal analysis, M.M., S.M. and F.U.; investigation, F.U.; resources, F.U.; data curation, F.U.; writing—original draft preparation, F.P., M.M., S.M., R.G. and F.U.; visualization, F.U.; supervision, F.U.; project administration, F.U.; funding acquisition, F.U. All authors have read and agreed to the published version of the manuscript.

Funding: This research received no external funding.

Institutional Review Board Statement: Not applicable.

Informed Consent Statement: Not applicable.

Data Availability Statement: The data presented in this study are available on request from the corresponding author (the Laboratory of Physiology carefully stores raw data to ensure permanent retention under a secure system).

Acknowledgments: The authors thank Vivatis Pharma GmbH (Hamburg, Germany) for kindly donating the substances necessary to conduct the research.

Conflicts of Interest: The authors, R.G. and F.P., were employed by Noivita Srls, and they had no role in interpreting the data. In addition, F.U. is a founder of Noivita Srls, and the company had no role in the design of the study; in the collection, analyses, or interpretation of data; in the writing of the manuscript; or in the decision to publish the results. The remaining authors declare that the research was conducted without commercial or financial relationships that could be construed as a potential conflict of interest. All of the collagen and hyaluronic acid formulations that were tested are commercially available ingredients. The manufacturers of these ingredients played no part in the design of the study, the collection or analysis of the data, the interpretation of the results, the preparation of the manuscript, or the decision to publish the study.

Abbreviations

The following abbreviations are used in this manuscript:

Adv-DMEM	Advanced Dulbecco's Modified Eagle Medium
ATCC	American Type Culture Collection
CD44	Cluster of Differentiation 44
COL1A1	Collagen Type I Alpha 1 Chain
DMEM	Dulbecco's Modified Eagle Medium
ECM	Extracellular Matrix
ELISA	Enzyme-Linked Immunosorbent Assay
ELN	Elastin
EMA	European Medicines Agency
FBS	Foetal Bovine Serum
FDA	Food and Drug Administration
GI	GreenIuronic
HA	Hyaluronic Acid
HAS2	Hyaluronan Synthase 2
MMP1	Matrix Metalloproteinase 1
MTT	3-(4,5-dimethylthiazol-2-yl)-2,5-diphenyltetrazolium bromide
PVDF	Polyvinylidene Fluoride
RHAMM	Receptor for Hyaluronan-Mediated Motility
RIPA	Radioimmunoprecipitation assay
ROS	Reactive Oxygen Species
SD	Standard Deviation
SDS-PAGE	Sodium Dodecyl Sulphate–Polyacrylamide Gel Electrophoresis
SH	Sodium Hyaluronate
TBS-T	Tris-buffered saline with Tween-20
TEER	Transepithelial Electrical Resistance
TJ	Tight Junctions
ZO-1	Zonula Occludens-1

Appendix A

Appendix A.1

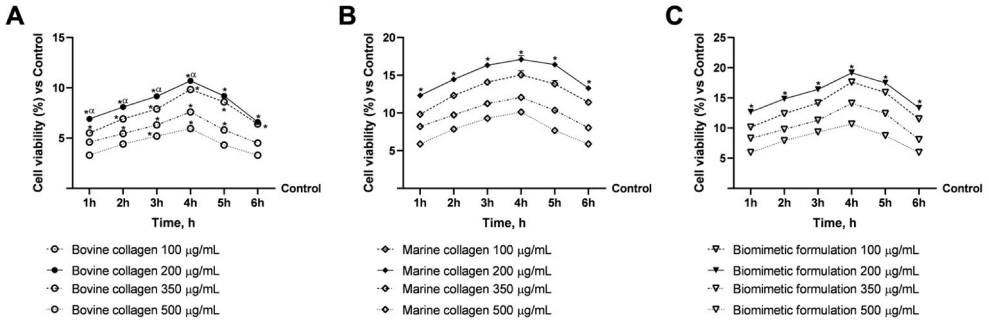


Figure A1. Concentration screening of the collagen hydrolysates and the biomimetic formulation on intestinal cells over time (from 1 h to 6 h). In (**A**), cell viability analysis of Bovine collagen was measured by the MTT test; in (**B**), cell viability analysis of Marine collagen was measured by the MTT test; and in (**C**), cell viability analysis of biomimetic formulation was measured by the MTT test. Results are expressed as mean ± SD (%) of five independent experiments conducted in triplicate. The asterisk (*) indicates a statistically significant difference compared with the control group.

Appendix A.2

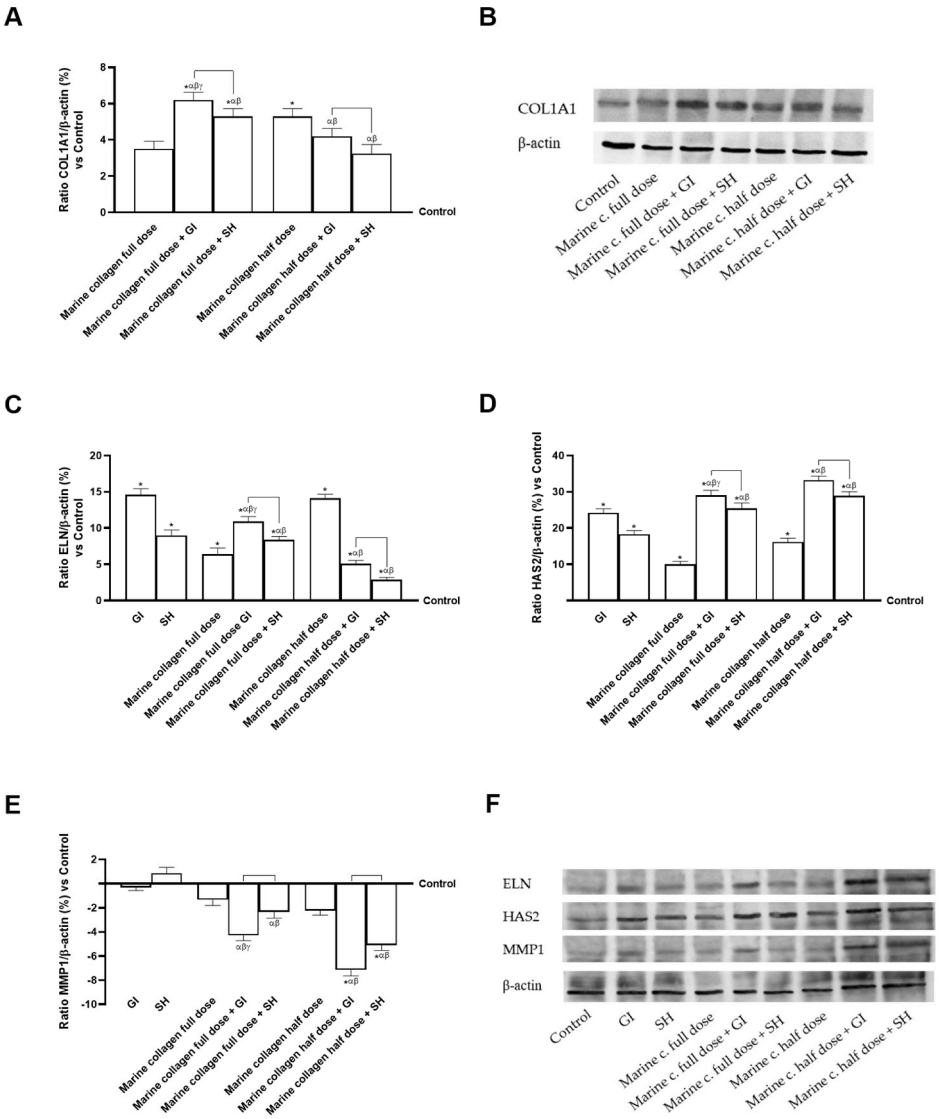


Figure A2. Western Blot Analysis of Marine collagen (c in panels B and F denotes collagen). In (**A**), the expression of COL1A1 protein; in (**B**), the representative gel lanes corresponding to the data shown in panel A; in (**C**) the relative expression (%) of ELN; in (**D**) the expression (%) of HAS2; in (**E**) the expression (%) of MMP1 and in (**F**), representative gel lanes corresponding to the data shown in panels (**C**–**E**). Results are expressed as mean ± SD (%) from three independent experiments, each performed in technical triplicate. The asterisk (*) indicates a statistically significant difference compared with the control group.

Appendix A.3

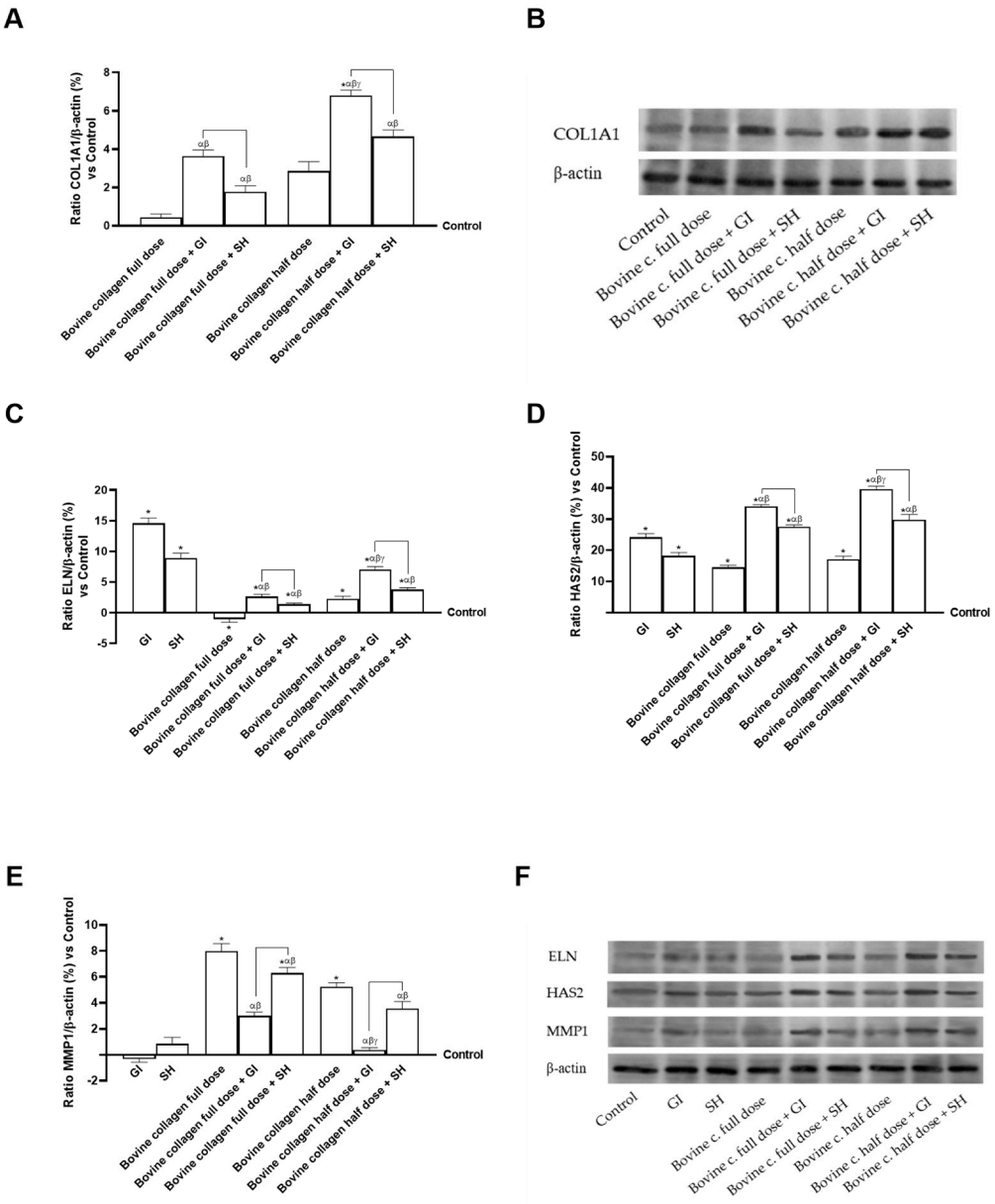


Figure A3. Western Blot Analysis of Bovine collagen (c in panels B and F denotes collagen). In (**A**), the expression of COL1A1 protein; in (**B**), the representative gel lanes corresponding to the data shown in panel A; in (**C**) the relative expression (%) of ELN; in (**D**) the expression (%) of HAS2; in (**E**) the expression (%) of MMP1 and in (**F**), representative gel lanes corresponding to the data shown in panels (**C**–**E**). Results are expressed as mean ± SD (%) from three independent experiments, each performed in technical triplicate. The asterisk (*) indicates a statistically significant difference compared with the control group.

Appendix A.4

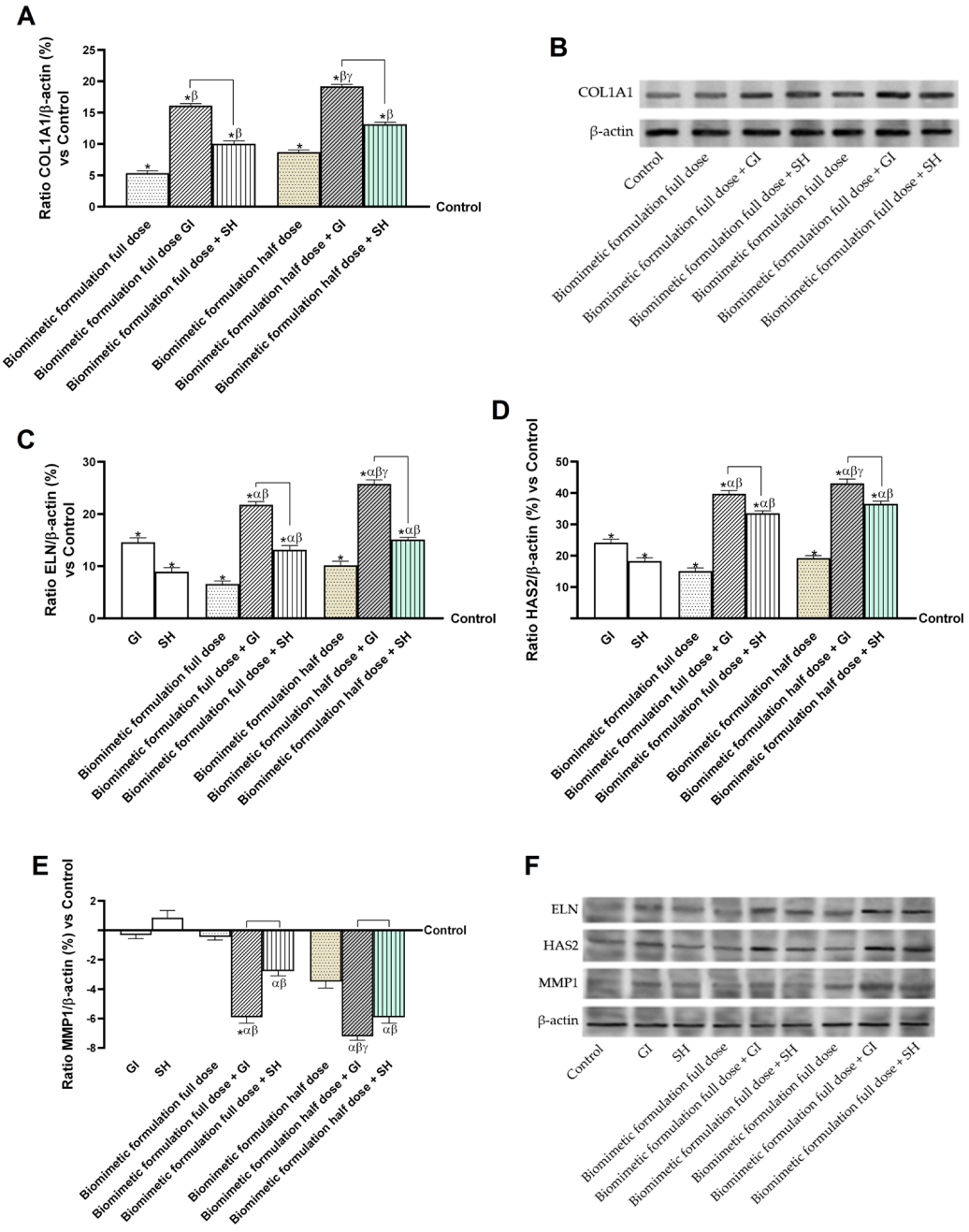


Figure A4. Western Blot Analysis of biomimetic formulation (c in panels B and F denotes collagen). In (**A**), the expression of COL1A1 protein; in (**B**), the representative gel lanes corresponding to the data shown in panel A; in (**C**) the relative expression (%) of ELN; in (**D**) the expression (%) of HAS2; in (**E**) the expression (%) of MMP1 and in (**F**), representative gel lanes corresponding to the data shown in panels (**C**–**E**). Results are expressed as mean ± SD (%) from three independent experiments, each performed in technical triplicate. The asterisk (*) indicates a statistically significant difference compared with the control group.

Appendix B

Appendix B.1

Table A1. The basolateral concentrations were determined experimentally in the basolateral compartment of the intestinal barrier model using an ELISA kit after 6 h of treatment. The data presented were expressed as the mean (µg/mL) of five independent experiments performed in triplicate.

Treatment	HA Initial Dose	Collagen Initial Dose	HA final Concentration µg/mL	Collagen Final Concentration µg/mL
Marine collagen full	-	200 µg/mL	-	38.0 ± 1.23
Marine collagen full + GI	10 µg/mL	200 µg/mL	2.06 ± 0.17	41.1 ± 1.26
Marine collagen full + SH	10 µg/mL	200 µg/mL	1.78 ± 0.12	35.7 ± 1.09
Marine collagen half	-	100 µg/mL	-	20.5 ± 0.95
Marine collagen half + GI	10 µg/mL	100 µg/mL	0.63 ± 0.03	6.25 ± 0.53
Marine collagen half + SH	10 µg/mL	100 µg/mL	0.49 ± 0.04	4.85 ± 0.37
Bovine collagen full	-	200 µg/mL	-	79.0 ± 1.85
Bovine collagen full + GI	10 µg/mL	200 µg/mL	2.02 ± 0.14	40.4 ± 1.20
Bovine collagen full + SH	10 µg/mL	200 µg/mL	1.64 ± 0.09	32.9 ± 0.96
Bovine collagen half	-	100 µg/mL	-	44.2 ± 1.31
Bovine collagen half + GI	10 µg/mL	100 µg/mL	4.22 ± 0.26	42.2 ± 1.32
Bovine collagen half + SH	10 µg/mL	100 µg/mL	3.47 ± 0.21	34.7 ± 0.97
biomimetic formulation full	-	200 µg/mL	-	7.27 ± 0.87
biomimetic formulation full + GI	10 µg/mL	200 µg/mL	1.50 ± 0.02	30.1 ± 0.86
biomimetic formulation full + SH	10 µg/mL	200 µg/mL	0.14 ± 0.005	2.81 ± 0.06
biomimetic formulation half	-	100 µg/mL	-	4.44 ± 0.29
biomimetic formulation half + GI	10 µg/mL	100 µg/mL	1.75 ± 0.08	17.5 ± 0.66
biomimetic formulation half + SH	10 µg/mL	100 µg/mL	0.95 ± 0.01	9.50 ± 0.71
GI	10 µg/mL	-	3.02 ± 0.19	-
SH	10 µg/mL	-	2.44 ± 0.15	-

Appendix B.2

Table A2. Hyaluronan- and hydroxyproline-equivalent material in the basolateral compartment after 6 h intestinal exposure. The data presented were expressed as the mean (µg/mL) of five independent experiments performed in triplicate.

Treatment	Hyaluronan (µg/mL)	Hydroxyproline (µg/mL)
Marine collagen full	-	4.33 ± 1.02
Marine collagen full + GI	1.65 ± 0.13	4.69 ± 1.07
Marine collagen full + SH	1.62 ± 0.11	4.07 ± 0.96
Marine collagen half	-	2.34 ± 0.91
Marine collagen half + GI	0.50 ± 0.05	0.71 ± 0.08
Marine collagen half + SH	0.45 ± 0.03	0.55 ± 0.06
Bovine collagen full	-	9.40 ± 0.71
Bovine collagen full + GI	1.62 ± 0.12	4.81 ± 0.44

Table A2. *Cont.*

Treatment	Hyaluronan (µg/mL)	Hydroxyproline (µg/mL)
Bovine collagen full + SH	1.49 ± 0.08	3.92 ± 0.37
Bovine collagen half	-	5.26 ± 0.68
Bovine collagen half + GI	3.38 ± 0.04	5.02 ± 0.64
Bovine collagen half + SH	3.16 ± 0.03	4.13 ± 0.56
biomimetic formulation full	-	0.058 ± 0.006
biomimetic formulation full + GI	1.20 ± 0.14	0.241 ± 0.01
biomimetic formulation full + SH	0.13 ± 0.01	0.022 ± 0.001
biomimetic formulation half	-	0.036 ± 0.002
biomimetic formulation half + GI	1.40 ± 0.16	0.140 ± 0.006
biomimetic formulation half + SH	0.86 ± 0.07	0.076 ± 0.003
GI	2.42 ± 0.27	-
SH	2.22 ± 0.24	-

Appendix B.3

Table A3. Direct comparison between GreenIuronic® (GI) and sodium hyaluronate (SH) for COL1A1 expression. Values are reported as mean ± SD for each formulation. Mean differences are calculated as GI minus SH and presented with their 95% confidence intervals and adjusted *p*-values. Positive differences indicate higher values in the GI-containing formulation, whereas negative differences indicate lower values.

Sample	Dose µg/mL	GI Mean ± SD	SH Mean ± SD	Mean Difference GI-SH (95% CI)	Adjusted *p* Value	n
Bovine Collagen	200	6.20 ± 0.42	5.30 ± 0.40	+0.90 (0.06 to 1.74)	0.041	3
Bovine Collagen	100	4.20 ± 0.40	3.25 ± 0.49	+0.95 (0.04 to 1.86)	0.045	3
Marine Collagen	200	3.63 ± 0.33	1.77 ± 0.31	+1.86 (1.20 to 2.52)	<0.001	3
Marine Collagen	100	6.80 ± 0.28	4.65 ± 0.36	+2.15 (1.50 to 2.80)	<0.001	3
biomimetic formulation	200	16.13 ± 0.45	10.03 ± 0.47	+6.10 (5.23 to 6.97)	<0.001	3
biomimetic formulation	100	19.22 ± 0.51	13.15 ± 0.34	+6.07 (5.40 to 6.73)	<0.001	3

Appendix B.4

Table A4. Direct comparison between GreenIuronic® (GI) and sodium hyaluronate (SH) for HAS2 expression. Values are reported as mean ± SD for each formulation. Mean differences are calculated as GI minus SH and presented with their 95% confidence intervals and adjusted *p*-values. Positive differences indicate higher values in the GI-containing formulation, whereas negative differences indicate lower values.

Sample	Dose µg/mL	GI Mean ± SD	SH Mean ± SD	Mean Difference GI-SH (95% CI)	Adjusted *p* Value	n
Bovine Collagen	200	29.00 ± 1.41	25.40 ± 1.56	+3.60 (0.56 to 6.64)	0.024	3
Bovine Collagen	100	33.25 ± 1.06	28.85 ± 1.20	+4.40 (2.00 to 6.80)	0.008	3
Marine Collagen	200	34.10 ± 0.57	27.60 ± 0.88	+6.50 (5.36 to 7.64)	<0.001	3
Marine Collagen	100	39.70 ± 0.85	29.80 ± 1.70	+9.90 (6.55 to 13.3)	<0.001	3
biomimetic formulation	200	39.75 ± 1.06	33.55 ± 0.78	+6.20 (4.17 to 8.23)	<0.001	3
biomimetic formulation	100	43.15 ± 1.34	36.55 ± 0.92	+6.60 (4.10 to 9.10)	<0.001	3

Appendix B.5

Table A5. Direct comparison between GreenIuronic® (GI) and sodium hyaluronate (SH) for MMP1 expression. Values are reported as mean ± SD for each formulation. Mean differences are calculated as GI minus SH and presented with their 95% confidence intervals and adjusted *p*-values. Positive differences indicate higher values in the GI-containing formulation, whereas negative differences indicate lower values.

Sample	Dose µg/mL	GI Mean ± SD	SH Mean ± SD	Mean Difference GI-SH (95% CI)	Adjusted *p* Value	n
Bovine Collagen	200	−4.30 ± 0.42	−2.35 ± 0.49	−1.95 (−2.9 to −1.04)	0.001	3
Bovine Collagen	100	−7.15 ± 0.49	−5.10 ± 0.42	−2.05 (−3.0 to −1.14)	0.009	3
Marine Collagen	200	3.00 ± 0.28	6.30 ± 0.41	−3.30 (−4.1 to −2.54)	<0.001	3
Marine Collagen	100	0.38 ± 0.18	3.58 ± 0.53	−3.20 (−4.0 to −2.41)	<0.001	3
biomimetic formulation	200	−5.90 ± 0.42	−2.78 ± 0.31	−3.12 (−3.8 to −2.41)	<0.001	3
biomimetic formulation	100	−7.20 ± 0.28	−5.90 ± 0.40	−1.30 (−2.0 to −0.64)	0.011	3

References

1. Amirrah, I.N.; Lokanathan, Y.; Zulkiflee, I.; Wee, M.F.M.R.; Motta, A.; Fauzi, M.B. A Comprehensive Review on Collagen Type I Development of Biomaterials for Tissue Engineering: From Biosynthesis to Bioscaffold. *Biomedicines* **2022**, *10*, 2307. [CrossRef] [PubMed]
2. Elango, J.; Hou, C.; Bao, B.; Wang, S.; Maté Sánchez de Val, J.E.; Wenhui, W. The Molecular Interaction of Collagen with Cell Receptors for Biological Function. *Polymers* **2022**, *14*, 876. [CrossRef] [PubMed]
3. Ivaskiene, T.; Viskelis, J.; Streimikyte, P.; Savickaitė, M.; Mobasheri, A.; Kaspute, G. Collagen Supplementation and Regenerative Health: Advances in Biomarker Detection and Smart Material Integration. *Front. Nutr.* **2025**, *12*, 1716166. [CrossRef] [PubMed]
4. Galvez-Martin, P.; Soto-Fernandez, C.; Romero-Rueda, J.; Cabañas, J.; Torrent, A.; Castells, G.; Martinez-Puig, D. A Novel Hyaluronic Acid Matrix Ingredient with Regenerative, Anti-Aging and Antioxidant Capacity. *Int. J. Mol. Sci.* **2023**, *24*, 4774. [CrossRef] [PubMed]
5. Wang, H. A Review of the Effects of Collagen Treatment in Clinical Studies. *Polymers* **2021**, *13*, 3868. [CrossRef] [PubMed]
6. Yuan, Z.; Memarzadeh, K.; Stephen, A.S.; Allaker, R.P.; Brown, R.A.; Huang, J. Development of a 3D Collagen Model for the In Vitro Evaluation of Magnetic-Assisted Osteogenesis. *Sci. Rep.* **2018**, *8*, 16270. [CrossRef] [PubMed]
7. Brandao-Rangel, M.A.R.; Oliveira, C.R.; da Silva Olímpio, F.R.; Aimbire, F.; Mateus-Silva, J.R.; Chaluppe, F.A.; Vieira, R.P. Hydrolyzed Collagen Induces an Anti-Inflammatory Response That Induces Proliferation of Skin Fibroblast and Keratinocytes. *Nutrients* **2022**, *14*, 4975. [CrossRef] [PubMed]
8. Liu, T.; Hao, J.; Lei, H.; Chen, Y.; Liu, L.; Jia, L.; Gu, J.; Kang, H.; Shi, J.; He, J.; et al. Recombinant Collagen for the Repair of Skin Wounds and Photo-Aging Damage. *Regen. Biomater.* **2024**, *11*, rbae108. [CrossRef] [PubMed]
9. Lim, Y.-S.; Ok, Y.-J.; Hwang, S.-Y.; Kwak, J.-Y.; Yoon, S. Marine Collagen as a Promising Biomaterial for Biomedical Applications. *Mar. Drugs* **2019**, *17*, 467. [CrossRef] [PubMed]
10. Jiao, S.; Zhang, X.; Cai, H.; Wu, S.; Ou, X.; Han, G.; Zhao, J.; Li, Y.; Guo, W.; Liu, T.; et al. Recent Advances in Biomimetic Hemostatic Materials. *Mater. Today Bio* **2023**, *19*, 100592. [CrossRef] [PubMed]
11. León-López, A.; Morales-Peñaloza, A.; Martínez-Juárez, V.M.; Vargas-Torres, A.; Zeugolis, D.I.; Aguirre-Álvarez, G. Hydrolyzed Collagen—Sources and Applications. *Molecules* **2019**, *24*, 4031. [CrossRef] [PubMed]
12. Avila Rodríguez, M.I.; Rodríguez Barroso, L.G.; Sánchez, M.L. Collagen: A Review on Its Sources and Potential Cosmetic Applications. *J. Cosmet. Dermatol.* **2018**, *17*, 20–26. [CrossRef] [PubMed]
13. Xu, Y.; Kirchner, M. Collagen Mimetic Peptides. *Bioengineering* **2021**, *8*, 5. [CrossRef] [PubMed]
14. Iaconisi, G.N.; Lunetti, P.; Gallo, N.; Cappello, A.R.; Fiermonte, G.; Dolce, V.; Capobianco, L. Hyaluronic Acid: A Powerful Biomolecule with Wide-Ranging Applications—A Comprehensive Review. *Int. J. Mol. Sci.* **2023**, *24*, 10296. [CrossRef] [PubMed]
15. Chylińska, N.; Maciejczyk, M. Hyaluronic Acid and Skin: Its Role in Aging and Wound-Healing Processes. *Gels* **2025**, *11*, 281. [CrossRef] [PubMed]
16. Misra, S.; Hascall, V.C.; Markwald, R.R.; Ghatak, S. Interactions between Hyaluronan and Its Receptors (CD44, RHAMM) Regulate the Activities of Inflammation and Cancer. *Front. Immunol.* **2015**, *6*, 201. [CrossRef] [PubMed]

17. Zerbinati, N.; Rauso, R.; Gonzalez, P.; Cherubino, M.; D'Este, E.; Calligaro, A.; Sommatis, S.; Maccario, C.; Mocchi, R. In Vitro Evaluation of Collagen Production on Human Fibroblasts Treated with Hyaluronic Acid PEG Cross-Linked with Micromolecules of Calcium Hydroxyapatite in Low Concentration. *J. Biol. Regul. Homeost. Agents* **2017**, *31*, 87–90. [PubMed]
18. Varì, S.; Minoretti, P.; Emanuele, E. Human Dermal Fibroblast Response to Hyaluronic Acid-Based Injectable Dermal Fillers: An In Vitro Study. *Postep. Dermatol. Alergol.* **2022**, *39*, 1088–1092. [CrossRef] [PubMed]
19. Osti, L.; Berardocco, M.; di Giacomo, V.; Di Bernardo, G.; Oliva, F.; Berardi, A.C. Hyaluronic Acid Increases Tendon-Derived Cell Viability and Collagen Type I Expression In Vitro. *BMC Musculoskelet. Disord.* **2015**, *16*, 284. [CrossRef] [PubMed]
20. Tavianatou, A.G.; Caon, I.; Franchi, M.; Piperigkou, Z.; Galesso, D.; Karamanos, N.K. Hyaluronan: Molecular Size-Dependent Signaling and Biological Functions in Inflammation and Cancer. *FEBS J.* **2019**, *286*, 2883–2908. [CrossRef] [PubMed]
21. Xu, Q.; Torres, J.E.; Hakim, M.; Babiak, P.M.; Pal, P.; Battistoni, C.M.; Nguyen, M.; Panitch, A.; Solorio, L.; Liu, J.C. Collagen- and Hyaluronic Acid-Based Hydrogels and Their Biomedical Applications. *Mater. Sci. Eng. R Rep.* **2021**, *146*, 100641. [CrossRef] [PubMed]
22. Ao, H.; Lin, C.; Nie, B.; Yang, S.; Xie, Y.; Wan, Y.; Zheng, X. The Synergistic Effect of Type I Collagen and Hyaluronic Acid on Titanium Coatings. *RSC Adv.* **2017**, *7*, 25828–25837. [CrossRef]
23. Mencarelli, N.; Arena, D.; Salamone, M.; Pietrangelo, L.; Berardi, A.C.; Cataldi, A.; Carradori, S.; Gallorini, M. The Combination of Hyaluronic Acids and Collagen Boosts Tendon-Derived Cell Response. *Inflamm. Res.* **2025**, *74*, 4. [CrossRef] [PubMed]
24. Mæhre, H.K.; Dalheim, L.; Edvinsen, G.K.; Elvevoll, E.O.; Jensen, I.J. Protein Determination—Method Matters. *Foods* **2018**, *7*, 5. [CrossRef] [PubMed]
25. Wu, L.; Liu, C.; Yao, T.; Shi, Y.; Shen, J.; Gao, X.; Qin, K. Structural and Compositional Changes in Two Marine Shell Traditional Chinese Medicines: A Comparative Analysis Pre- and Post-Calcination. *J. AOAC Int.* **2024**, *107*, 704–713. [CrossRef] [PubMed]
26. Inacio, P.A.Q.; Chaluppe, F.A.; Aguiar, G.F.; Coelho, C.F.; Vieira, R.P. Effects of Hydrolyzed Collagen as a Dietary Supplement on Fibroblast Activation: A Systematic Review. *Nutrients* **2024**, *16*, 1543. [CrossRef] [PubMed]
27. Xin, X.Y.; Zhou, J.; Liu, G.G.; Zhang, M.-Y.; Li, X.-Z.; Wang, Y. Anti-Inflammatory Activity of Collagen Peptide In Vitro and Its Effect on Improving Ulcerative Colitis. *npj Sci. Food* **2025**, *9*, 1. [CrossRef] [PubMed]
28. Galla, R.; Mulè, S.; Ferrari, S.; Molinari, C.; Uberti, F. Non-Animal Hyaluronic Acid and Probiotics Enhance Skin Health via the Gut–Skin Axis: An In Vitro Study on Bioavailability and Cellular Impact. *Int. J. Mol. Sci.* **2025**, *26*, 897. [CrossRef] [PubMed]
29. Uberti, F.; Mulè, S.; Parini, F.; Musu, M.; Galla, R. Natural Extract Combination Modulates Intestinal Barrier and Hepatic Cholesterol via the Gut–Liver Axis In Vitro. *Pharmaceutics* **2026**, *18*, 328. [CrossRef] [PubMed]
30. Galla, R.; Ruga, S.; Aprile, S.; Ferrari, S.; Brovero, A.; Grosa, G.; Molinari, C.; Uberti, F. New Hyaluronic Acid from Plant Origin to Improve Joint Protection. *Int. J. Mol. Sci.* **2022**, *23*, 8114. [CrossRef] [PubMed]
31. Cho, J.; Bejaoui, M.; Isoda, H. Regulation of Keratinocyte Proliferation and Differentiation by Secoiridoid Oleacein in Monoculture and Fibroblast Co-Culture Models. *Biomed. Pharmacother.* **2025**, *185*, 117985. [CrossRef] [PubMed]
32. Galla, R.; Grisenti, P.; Farghali, M.; Saccuman, L.; Ferraboschi, P.; Uberti, F. Ovotransferrin Supplementation Improves the Iron Absorption: An In Vitro Gastro-Intestinal Model. *Biomedicines* **2021**, *9*(11), 1543. [CrossRef] [PubMed]
33. Guha, S.; Alvarez, S.; Majumder, K. Transport of Dietary Anti-Inflammatory Peptide, γ-Glutamyl Valine (γ-EV), across the Intestinal Caco-2 Monolayer. *Nutrients* **2021**, *13*, 1448. [CrossRef] [PubMed]
34. Galla, R.; Ferrari, S.; Miletto, I.; Mulè, S.; Uberti, F. In Vitro Neuroprotective Effects of a Mixed Extract of Bilberry, *Centella asiatica*, *Hericium erinaceus*, and Palmitoylethanolamide. *Foods* **2025**, *14*(15), 2678. [CrossRef] [PubMed]
35. Morsanuto, V.; Galla, R.; Molinari, C.; Uberti, F. A New Palmitoylethanolamide Form Combined with Antioxidant Molecules to Improve Its Effectivess on Neuronal Aging. *Brain Sci.* **2020**, *10*, 457. [CrossRef] [PubMed]
36. Tahri, S.; Maarof, M.; Masri, S.; Che Man, R.; Masmoudi, H.; Fauzi, M.B. Keratinocytes and Fibroblasts Interactions in 3D Model. *Front. Bioeng. Biotechnol.* **2023**, *11*, 1200618. [CrossRef] [PubMed]
37. Ruga, S.; Galla, R.; Ferrari, S.; Invernizzi, M.; Uberti, F. Novel Approach to the Treatment of Neuropathic Pain Using a Combination with Palmitoylethanolamide and *Equisetum arvense* L. in an In Vitro Study. *Int. J. Mol. Sci.* **2023**, *24*, 5503. [CrossRef] [PubMed]
38. Wu, Y.; Jiang, Y.; Xiao, B.; Xie, L.; Zhou, N.; Zeng, A.; Liu, C. TFR1 as Biomarker of Pulmonary Fibrosis. *Int. J. Chron. Obstruct. Pulmon. Dis.* **2025**, *20*, 2715–2725. [CrossRef] [PubMed]
39. Yue, X.; Tiwari, N.; Zhu, L.; Ngo, H.D.T.; Lim, J.M.; Gim, B.; Jing, S.; Wang, Y.; Qian, Y.; Lee, I. Tankyrase-1-Mediated Degradation of Golgin45 Regulates Glycosyltransferase Trafficking and Protein Glycosylation in a Rab2-GTP-Dependent Manner. *Commun. Biol.* **2021**, *4*, 1370. [CrossRef] [PubMed]
40. Aborehab, N.M.; El Bishbishy, M.H.; Refaiy, A.; Waly, N.E. A Putative Chondroprotective Role for IL-1β and MPO in Herbal Treatment of Experimental Osteoarthritis. *BMC Complement. Altern. Med.* **2017**, *17*, 495. [CrossRef] [PubMed]
41. Hussein, R.S.; Bin Dayel, S.; Abahussein, O.; El-Sherbiny, A.A. Influences on Skin and Intrinsic Aging: Biological, Environmental, and Therapeutic Insights. *J. Cosmet. Dermatol.* **2025**, *24*, e16688. [CrossRef] [PubMed]

42. Dewi, D.A.R.; Arimuko, A.; Norawati, L.; Yenny, S.W.; Setiasih, N.L.; Perdiyana, A.; Arkania, N.; Nadhira, F.; Wiliantari, N. Exploring the Impact of Hydrolyzed Collagen Oral Supplementation on Skin Rejuvenation: A Systematic Review and Meta-Analysis. *Cureus* **2023**, *15*, e50231. [CrossRef] [PubMed]
43. Song, W.; Chen, Q.; Wang, Y.; Han, Y.; Zhang, H.; Li, B.; Yu, G. Structure–Activity Relationship of Collagen Peptides. *Mar. Drugs* **2019**, *17*, 450. [CrossRef] [PubMed]
44. Chen, Q.; Chen, O.; Martins, I.M.; Hou, H.; Zhao, X.; Blumberg, J.B.; Li, B. Collagen Peptides Ameliorate Epithelial Barrier Dysfunction. *Food Funct*. **2017**, *8*, 1144–1151. [CrossRef] [PubMed]
45. Saturnino, C.; Sinicropi, M.S.; Parisi, O.I.; Iacopetta, D.; Popolo, A.; Marzocco, S.; Autore, G.; Caruso, A.; Cappello, A.R.; Longo, P.; et al. Acetylated Hyaluronic Acid: Enhanced Bioavailability and Biological Studies. *Biomed. Res. Int*. **2014**, *2014*, 921549. [CrossRef] [PubMed]
46. Dierckx, S.; Patrizi, M.; Merino, M.; González, S.; Mullor, J.L.; Nergiz-Unal, R. Collagen Peptides Affect Collagen Synthesis and the Expression of Collagen, Elastin, and Versican Genes in Cultured Human Dermal Fibroblasts. *Front. Med*. **2024**, *11*, 1397517. [CrossRef] [PubMed]
47. Avila-Martinez, N.; Pfirrmann, M.; Gomes, M.L.N.P.; Krymchenko, R.; Versteeg, E.M.M.; Vlig, M.; Verdoes, M.; van Kuppevelt, T.H.; Boekema, B.K.H.L.; Daamen, W.F. Effect of Hyaluronan in Collagen Biomaterials on Human Macrophages and Fibroblasts In Vitro. *J. Funct. Biomater.* **2025**, *16*, 167. [CrossRef] [PubMed]
48. Marinho, A.; Nunes, C.; Reis, S. Hyaluronic Acid: A Key Ingredient in the Therapy of Inflammation. *Biomolecules* **2021**, *11*, 1518. [CrossRef] [PubMed]
49. Zhu, S.; Liu, Y.; Li, Y.; Guo, X.; Zhao, Z.; Yu, J.; Zhao, L.; She, W.; Zeng, M.; Li, S.; et al. Collagen Peptides Ameliorate Murine Chronic Colitis: Toward the Molecular Basis for Their Enhancement of Intestinal Epithelial Defenses Against Oxidative Stress. *Mol. Nutr. Food Res*. **2025**, *69*, e70177. [CrossRef] [PubMed]
50. Salem, I.; Ramser, A.; Isham, N.; Ghannoum, M.A. The Gut Microbiome as a Major Regulator of the Gut-Skin Axis. *Front. Microbiol*. **2018**, *9*, 1459. [CrossRef] [PubMed]
51. Shoulders, M.D.; Raines, R.T. Collagen Structure and Stability. *Annu. Rev. Biochem*. **2009**, *78*, 929–958. [CrossRef] [PubMed]
52. Ricard-Blum, S. The Collagen Family. *Cold Spring Harb. Perspect. Biol*. **2011**, *3*, a004978. [CrossRef] [PubMed]
53. Zague, V. Effects of Collagen Hydrolysate Intake on Skin. *Arch. Dermatol. Res*. **2008**, *300*, 479–483. [CrossRef] [PubMed]
54. Asserin, J.; Lati, E.; Shioya, T.; Prawitt, J. The Effect of Oral Collagen Peptide Supplementation on Skin Moisture and the Dermal Collagen Network: Evidence from an Ex Vivo Model and Randomized, Placebo-Controlled Clinical Trials. *J. Cosmet. Dermatol*. **2015**, *14*, 291–301. [CrossRef] [PubMed]
55. Kielty, C.M.; Sherratt, M.J.; Shuttleworth, C.A. Elastic Fibres. *J. Cell Sci*. **2002**, *115*, 2817–2828. [CrossRef] [PubMed]
56. Abe, M.; Masuda, M.; Mizukami, Y.; Inoue, S.; Mizutani, Y. Epidermal Keratinocytes Regulate Hyaluronan Metabolism via Extracellularly Secreted Hyaluronidase 1 and Hyaluronan Synthase 3. *J. Biol. Chem*. **2024**, *300*, 107449. [CrossRef] [PubMed]
57. Santini, A.; Cammarata, S.M.; Capone, G.; Ianaro, A.; Tenore, G.C.; Pani, L.; Novellino, E. Nutraceuticals: Opening the Debate for a Regulatory Framework. *Br. J. Clin. Pharmacol*. **2018**, *84*, 659–672. [CrossRef] [PubMed]

Disclaimer/Publisher's Note: The statements, opinions and data contained in all publications are solely those of the individual author(s) and contributor(s) and not of MDPI and/or the editor(s). MDPI and/or the editor(s) disclaim responsibility for any injury to people or property resulting from any ideas, methods, instructions or products referred to in the content.